Allosteric and covalent strategies for RAS-driven cancers from KRAS G12C to pan-RAS inhibition

Norliyana Amran [1]*, Heshu Rahman [2]

Abstract

RAS was regarded for nearly three decades as the archetypal “undruggable” therapeutic target. Its picomolar affinity for nucleotides, the millimolar concentration of intracellular GTP, and the absence of an apparent ligandable pocket on its protein surface made direct pharmacological inhibition seem not merely challenging but virtually infeasible. This prevailing view was ultimately overturned by the identification of a cryptic pocket beneath the Switch II region and the recognition that a mutation-introduced cysteine could provide a tractable site for covalent inhibitor engagement. This review traces what has followed. Covalent OFF-state inhibitors validated mutant RAS as a drug target and reached the clinic, but they remain confined to KRAS G12C, an allele that is common in lung cancer and scarce in the pancreatic and colorectal tumours where RAS mutation is nearly universal. The field's response has been to stop waiting for the inactive state. Non-covalent allele-selective agents engage Switch II without a reactive handle; tri-complex molecular glues co-opt cyclophilin A to occlude the effector interface on active RAS across alleles and isoforms; targeted degraders remove the protein outright; nucleotide-free trappers intercept the apo intermediate during exchange. Randomised Phase III data now support pan-RAS inhibition in pretreated metastatic pancreatic cancer. Resistance, predictably, has followed, and its architecture is instructive: on-target pocket and glue-interface mutations, effector-level competition, copy-number gain, and non-genetic bypass through YAP/TAZ-TEAD and lineage plasticity. We synthesise structural, preclinical, and clinical evidence across these modalities, examine where the data remain thin, and argue that durability will depend less on potency than on biomarker-guided combinations chosen against the escape route a given tumour is likely to take.

Keywords

RAS; KRAS; allosteric inhibition; Switch-II pocket; tri-complex molecular glue; cyclophilin A; targeted protein degradation; pancreatic ductal adenocarcinoma; drug resistance

1. Introduction

Few oncogenes carry the epidemiological burden that RAS does. The family comprises KRAS, NRAS, and HRAS, and mutations in one of them are found in something close to 30% of all human cancers, with KRAS alone accounting for roughly 75% to 86% of RAS-mutant tumours (Alanazi et al., 2025; Prior et al., 2020). What gives those aggregate figures their clinical force is their tissue distribution, which is strikingly uneven. KRAS is

Significance | Allosteric targeting of active-state and apo RAS extends effective therapy beyond G12C to the alleles driving pancreatic and colorectal cancer.

Correspondence.

Norliyana Amran, Department of Pharmaceutical Chemistry, School of Pharmaceutical Sciences, Universiti Sains Malaysia, Penang, Malaysia. E-mail: liyana_amran@yahoo.com.

Editor Muhammad Asif, Ph.D. And accepted by the Editorial Board Oct 29, 2026 (received for review Sep 2, 2026)

Author Affiliation:

[1] Department of Pharmaceutical Chemistry, School of Pharmaceutical Sciences, Universiti Sains Malaysia, Penang, Malaysia.

[2] Department of Medical Laboratory Sciences, College of Health Sciences, Komar University of Science and Technology, Chaq Chaq Qularaese, Sulaimani City, Kurdistan Region, Northern Iraq.

Please cite this article as: Amran, N., Rahman, H. (2026). "Allosteric and covalent strategies for RAS-driven cancers from KRAS G12C to pan-RAS inhibition", Integrative Biomedical Research, 10(2), 1-24, 10959

3068-6326/© 2026 (Integrative Biomedical Research), a publication of Eman Research, USA.
This is an open access article under the CC BY-NC-ND license.
(http://creativecommons.org/licenses/by-nc-nd/4.0/)
(https://publishing.emanresearch.org)

altered in more than 90% of pancreatic ductal adenocarcinomas (PDAC), about 40% of colorectal cancers (CRC), and roughly 30% of non-small cell lung cancers (NSCLC) (Chan et al., 2026; Prior et al., 2020). In PDAC, where five-year survival still sits below 12%, mutant KRAS is not one driver among several but the initiating event, and it shapes everything downstream of itself: proliferation, metabolic rewiring, the dense desmoplastic stroma, and an immunosuppressive microenvironment that has defeated most immunotherapeutic approaches tried against it (Ahmed et al., 2026; Alanazi et al., 2025).

Point mutation is not the only route to pathological RAS activity. Wild-type isoforms can be driven into sustained signalling by overexpressed or mutated receptor tyrosine kinases, by amplification of the KRAS locus itself, or by loss of negative regulators such as NF1 (Alanazi et al., 2025; Camps-Fajol et al., 2025). The practical implication is that the therapeutic problem is broader than the mutational one, and it argues, as we discuss later, for agents that do not depend on a particular substitution being present. Either way, neutralising RAS output has remained the highest-value unsolved problem in precision oncology for as long as the field has existed (Choucair et al., 2025).

RAS proteins are small GTPases that operate as binary switches, cycling between an inactive GDP-bound state and an active GTP-bound state (Alanazi et al., 2025; Camps-Fajol et al., 2025). Guanine nucleotide exchange factors such as SOS1 catalyse GDP release and permit GTP loading; GTPase-activating proteins such as NF1 accelerate the intrinsically sluggish hydrolysis that returns the protein to rest (Camps-Fajol et al., 2025). The conserved G-domain holds the nucleotide pocket together with two flexible elements, Switch I at residues 30 to 40 and Switch II at residues 59 to 76, whose conformation determines whether effectors can engage (Alanazi et al., 2025; L. Jiang et al., 2025). Oncogenic substitutions cluster at G12, G13, and Q61 and sabotage this cycle in two distinguishable ways: bulk at glycine 12 or 13 obstructs insertion of the GAP catalytic arginine finger, while substitution at glutamine 61 displaces the water molecule required for cleavage (Chan et al., 2026). Either way the protein remains GTP-loaded, and in that state it binds RAF kinases, the PI3K p110 subunit, and RALGDS, relaying continuous proliferative and survival signals (Camps-Fajol et al., 2025). This cycle, and the way mutation subverts it..

The pharmacological obstacles followed directly from that biochemistry. RAS binds GTP and GDP with picomolar to nanomolar affinity, and cytosolic GTP sits near 0.5 mM, so nucleotide-competitive inhibition was never a realistic proposition (Alanazi et al., 2025; Camps-Fajol et al., 2025). Compounding this, crystallographic surveys showed a smooth, shallow protein surface with no deep hydrophobic cavity of the kind medicinal chemistry normally requires (Alanazi et al., 2025). The verdict of undruggability was, given the evidence available at the time, reasonable rather than negligent, which is worth saying because it illustrates how a well-supported structural conclusion can still be overturned by finding a state nobody had looked for.

That overturning came in 2013, when Ostrem and colleagues identified a cryptic, transient pocket beneath the Switch II region, now designated the Switch-II pocket (Ostrem et al., 2013). The pocket is not obvious in the ground-state structure; it opens as the protein breathes, and it sits close enough to residue 12 that a molecule occupying it can be tethered by a covalent bond to the cysteine supplied by the G12C mutation (Ostrem et al., 2013). Compounds built on this logic bind the inactive GDP-bound conformation preferentially, shift the equilibrium toward it, and prevent effector engagement (Canon et al., 2019; Janes et al., 2018). Sotorasib and adagrasib carried the approach through to regulatory approval in 2021 and 2022 for pretreated KRAS G12C NSCLC (Jänne et al., 2022; Skoulidis et al., 2021), with randomised confirmation against docetaxel following shortly afterwards (de Langen et al., 2023).

The proof of concept was genuine and, in our reading, more important than the clinical magnitude of the benefit. But three limitations became apparent quickly. G12C accounts for about 13% of NSCLC yet only 3% to 4% of CRC and 1% to 3% of PDAC, so the modality misses the tumours in which RAS mutation matters most (Alanazi et al., 2025; Chan et al., 2026). Non-G12C variants offer no reactive handle, and the dominant PDAC alleles G12D and G12V favour the GTP-bound state so strongly that the inactive population an OFF-state drug depends upon is scarce (Chan et al., 2026; Isermann et al., 2025). Finally, responses erode through secondary pocket mutations such as Y96C and H95D/Q/R, through KRAS amplification, and through rapid RTK-SHP2-SOS1 feedback that reloads wild-type or newly synthesised RAS

with GTP (Awad et al., 2021; Isermann et al., 2025; Tanaka et al., 2021; Zhao et al., 2021).

The response to those limitations has been an unusually rapid diversification of chemical strategy, and it is that diversification this review examines. Rather than treating each modality in isolation, we have tried to organise them by the conformational state they exploit, because that choice determines almost everything else about an agent's allele breadth, its resistance liabilities, and where it fits in a combination. Our objectives are to (i) set out the structural and conformational logic of the RAS switch and how hotspot mutations subvert it; (ii) trace the evolution of allosteric discovery from the Switch-II pocket through non-covalent allele-selective inhibitors, degraders, and nucleotide-free trappers, as summarised in; (iii) analyse the mechanism and clinical translation of active-state multi-selective tri-complex inhibitors, including the randomised Phase III evidence now available in PDAC; and (iv) examine resistance architecture and the biomarker-guided combination frameworks being built against it. We have tried to be explicit about the difference between what has been demonstrated in randomised trials, what rests on single-arm data, and what remains preclinical, because in a field moving this quickly those distinctions blur easily.

2. From a Cryptic Pocket to State-Selective Pharmacology

2.1. Structural biochemistry of the RAS switch

Any account of RAS pharmacology has to begin with conformational dynamics, because the druggability of this protein turns out to be a property of particular states rather than of the protein as a whole (Alanazi et al., 2025; Camps-Fajol et al., 2025). The G-domain houses the nucleotide-binding site and the two switch loops; nucleotide identity determines their ordering, and their ordering determines effector competence (L. Jiang et al., 2025). In the GTP-bound state, Switch I and Switch II adopt the arrangement that RAF, PI3K, and RALGDS recognise. In the GDP-bound state, they relax into a conformation that effectors cannot productively bind. The cycle between them is not spontaneous on any useful timescale; it is driven by GEFs such as SOS1 in one direction and GAPs such as NF1 in the other (Camps-Fajol et al., 2025). (Figure 2) summarises this architecture.

Oncogenic substitutions do not create a new signalling function. They disable the return leg of the cycle. G12 and G13 substitutions introduce steric bulk that prevents the GAP arginine finger from reaching the catalytic centre, while Q61 substitutions remove the positioning of the nucleophilic water (Chan et al., 2026). Both intrinsic and GAP-stimulated hydrolysis are therefore impaired, and the switch accumulates in the ON state (Alanazi et al., 2025). It is worth noting that these alleles are not interchangeable. G12D and G12V sustain higher GTP occupancy than G12C, G12R has distinct effector preferences, and Q61 variants differ again in their hydrolysis defect (Chan et al., 2026; Isermann et al., 2025). Much of the clinical heterogeneity discussed later traces back to these biochemical differences rather than to tissue context alone.

2.2. The Switch-II pocket and first-generation OFF-state covalent inhibitors

The pocket that broke the deadlock is cryptic in the strict sense: it is not present in the apo or ground-state structures used in earlier docking campaigns, and it becomes occupiable only transiently (Ostrem et al., 2013). This matters methodologically. A structure-based programme searching static coordinates would not have found it, and the discovery depended on covalent fragment screening against the mutant protein rather than on computational prediction. Once identified, the pocket could be exploited with molecules that occupy it while forming an irreversible adduct with Cys12, trapping the protein in the GDP state and preventing exchange (Janes et al., 2018; Ostrem et al., 2013).

Clinical development followed quickly. Sotorasib produced objective response rates of roughly 37% with median progression-free survival near 6.8 months in pretreated G12C NSCLC (Skoulidis et al., 2021), and adagrasib performed comparably at around 43% (Jänne et al., 2022); randomised comparison against docetaxel confirmed a progression-free survival advantage (de Langen et al., 2023). Divarasib, glecirasib, olomorasib, and garsorasib have since broadened the class (Li et al., 2024; Sacher et al., 2023). The pharmacological properties of these agents are compared in (Table 1) and their trial outcomes in (Table 2).

Yet the ceiling was visible almost immediately. Allele restriction confines the class to a minority of RAS-mutant disease, concentrated in lung cancer (Alanazi et al., 2025). Dependence on the inactive state is a second

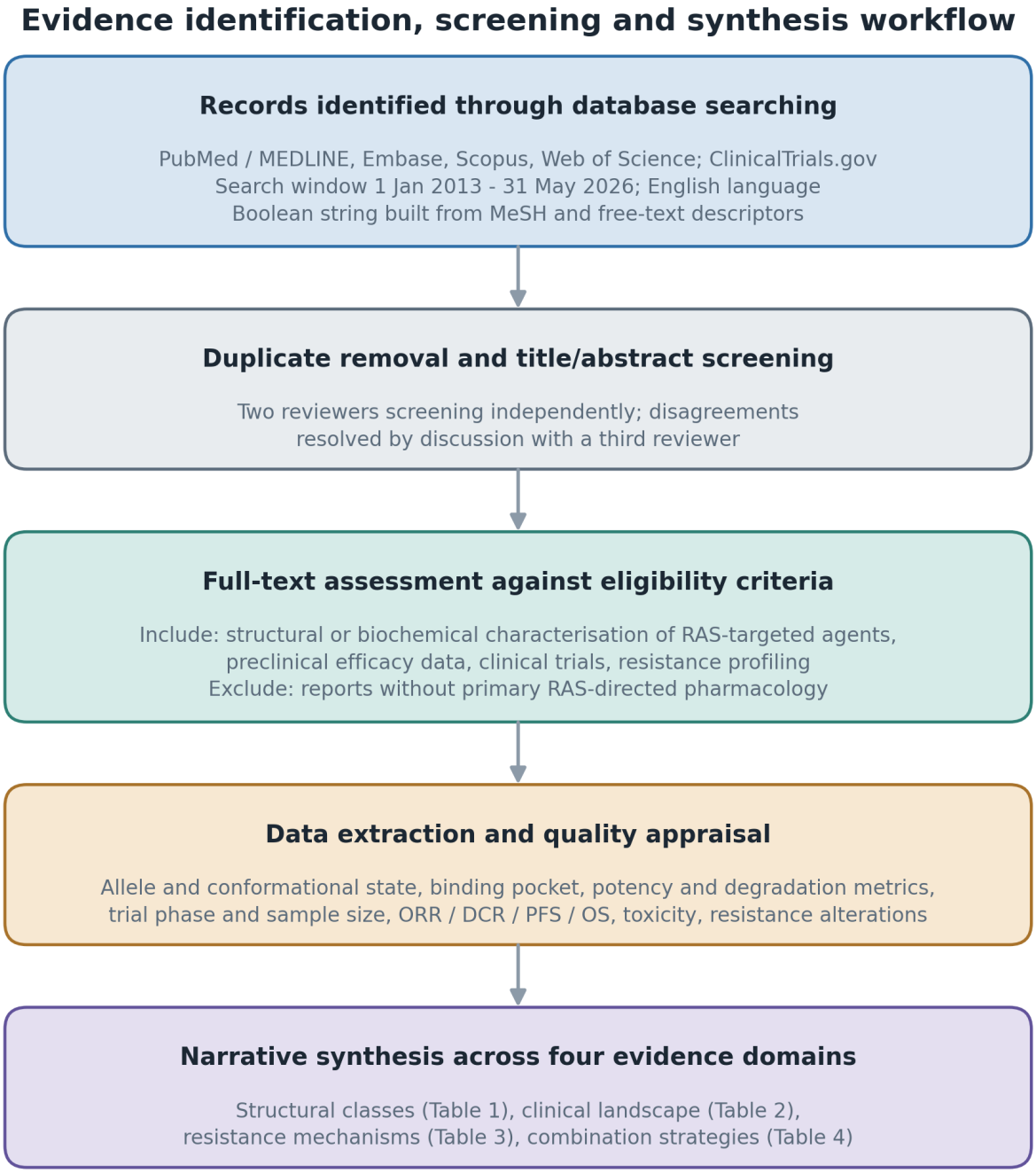


Figure 1. Evidence identification, screening and synthesis workflow used in this review. The diagram follows records from database identification through to narrative synthesis, naming at each stage the decisions that determined which evidence entered the review. Searches covered PubMed/MEDLINE, Embase, Scopus and Web of Science, supplemented by ClinicalTrials.gov and the abstract archives of AACR, ASCO and ESMO, for the period 1 January 2013 to 31 May 2026. Screening and full-text assessment were performed independently by two reviewers with a third adjudicating disagreements, and eligibility required a direct RAS-binding component rather than downstream pathway inhibition alone. Extracted data were grouped into the four evidence domains corresponding to Tables 1 to 4.

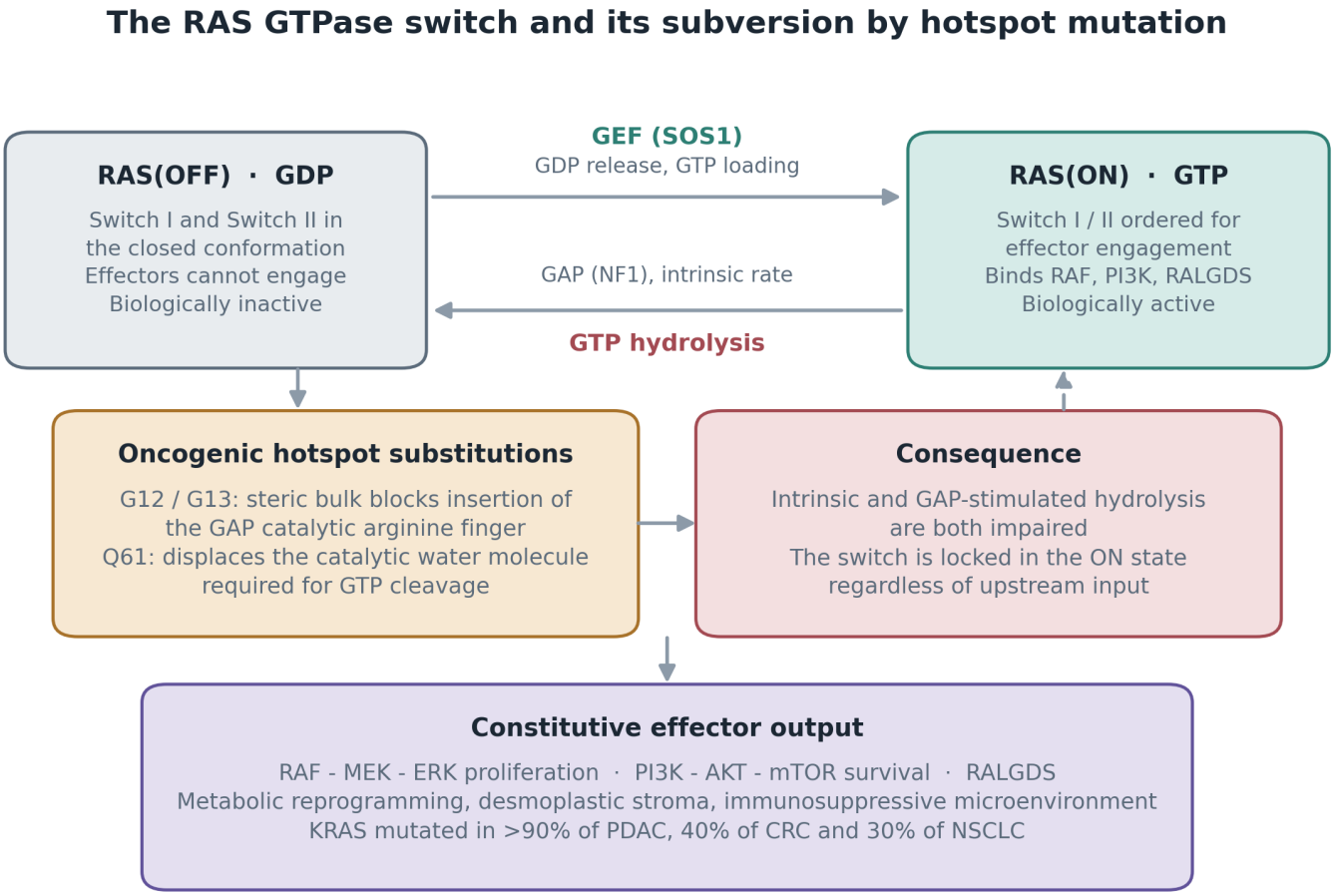


Figure 2. The RAS GTPase switch and its subversion by hotspot mutation. The upper panel shows the physiological cycle between the inactive GDP-bound and active GTP-bound conformations, driven forward by guanine nucleotide exchange factors such as SOS1 and reversed by GTPase-activating proteins such as NF1 acting on an intrinsically slow hydrolysis reaction. The lower panels show how oncogenic substitution breaks the return leg: bulk at glycine 12 or 13 obstructs insertion of the GAP catalytic arginine finger, while substitution at glutamine 61 displaces the water molecule required for cleavage. Both intrinsic and GAP-stimulated hydrolysis are therefore impaired and the switch accumulates in the active state, sustaining effector output through RAF-MEK-ERK, PI3K-AKT-mTOR and RALGDS.

constraint, and a subtle one: the drug can only act on protein that happens to be GDP-loaded, so alleles with fast nucleotide cycling or high intrinsic GTP occupancy present a smaller target population (Chan et al., 2026; Isermann et al., 2025). Resistance is the third. Secondary Switch-II mutations, KRAS amplification, and adaptive RTK feedback all restore signalling, and non-genetic mechanisms including epithelial-mesenchymal transition add a further layer (Adachi et al., 2020; Awad et al., 2021; Isermann et al., 2025; Tanaka et al., 2021).

2.3. Non-covalent allele-selective inhibition beyond G12C

Extending allele-selective targeting past G12C meant engaging Switch II without a reactive cysteine, which is a harder medicinal chemistry problem because all the binding energy has to come from non-covalent contacts. MRTX1133 showed it could be done, exploiting salt bridges and an extensive hydrogen-bonding network with the mutant aspartate at position 12 to achieve sub-picomolar affinity while stabilising an inactive-like conformation (Hallin et al., 2022; X. Wang et al., 2022). In G12D-driven PDAC models it suppressed ERK phosphorylation and produced regression of at least 30% in roughly three-quarters of models tested (Hallin et al., 2022).

What proved equally interesting was the effect on the microenvironment. MRTX1133 depleted myeloid-derived suppressor cells, repolarised tumour-associated macrophages toward an M1 phenotype, increased intratumoural CD8+ T-cell infiltration, and reprogrammed cancer-associated fibroblasts (Hallin et al., 2022). Whether these changes are a direct consequence of RAS inhibition in tumour cells or a secondary effect of tumour regression is not fully settled, and the distinction matters for how such agents are combined with immunotherapy. MRTX1133 itself was discontinued for formulation reasons rather than lack of activity, but it established the concept, and clinical-stage successors including HRS-4642, GFH375, INCB161734, and TSN1611 have followed (Chan et al., 2026). HRS-4642 combined with gemcitabine and nab-paclitaxel produced a confirmed response rate of 60% in treatment-naive G12D PDAC in Phase Ib/II evaluation (L. Wang et al., 2025), a figure that would have seemed implausible in this disease a decade ago, though single-arm data at that stage warrant caution.

2.4. Active-state tri-complex molecular glues

The conceptual break with earlier work came from abandoning the inactive state altogether. If the oncogenic problem is that RAS is stuck ON, then waiting for it to cycle OFF in order to drug it is, on reflection, a strange requirement to impose. Tri-complex inhibitors instead engage the GTP-bound conformation directly and recruit the abundant endogenous chaperone cyclophilin A to form a synthetic ternary assembly (Holderfield et al., 2024; Schulze et al., 2023). The bulk of the recruited chaperone projects across the Switch I and Switch II surface, physically excluding RAF and PI3K without the drug itself needing to occupy the effector site or to react with a cysteine (Schulze et al., 2023). The mechanism is set out in (Figure 4).

Because the recognition element is the active conformation rather than a mutant side chain, the approach generalises across G12D, G12V, G12R, G12C, G13D, and Q61H, and across KRAS, NRAS, and HRAS including wild-type isoforms (Holderfield et al., 2024). Daraxonrasib (RMC-6236), an oral non-covalent multi-selective agent, produced deep and durable regressions across PDAC, NSCLC, and CRC models (Cregg et al., 2025; J. Jiang et al., 2024) and disease control rates of 85% to 87% in early clinical evaluation (Arbour et al., 2023). RMC-7977 served as the preclinical tool compound establishing tolerability of concurrent wild-type and mutant inhibition (Holderfield et al., 2024; Wasko et al., 2024). Zoldonrasib (RMC-9805) and elironrasib (RMC-6291) apply the same logic covalently and allele-selectively, to active G12D and G12C respectively (Schulze et al., 2023; Spira et al., 2025).

The obvious concern with pan-RAS inhibition is therapeutic index, since wild-type RAS is required in normal tissue. In practice the toxicity profile has been manageable, dominated by rash and stomatitis rather than by the catastrophic effects one might have predicted (O'Reilly et al., 2026; Wasko et al., 2024). Why the window exists is not fully explained; differential dependence of tumour versus normal tissue on RAS output is the usual explanation, and it is plausible, but we would treat it as a description rather than a mechanism. Resistance has also emerged with a distinctive signature, discussed in Section 2.6 and tabulated in (Table 3).

2.5. Targeted degradation and nucleotide-free trapping

2.5.1. Event-driven degradation

Proteolysis-targeting chimeras shift the pharmacology

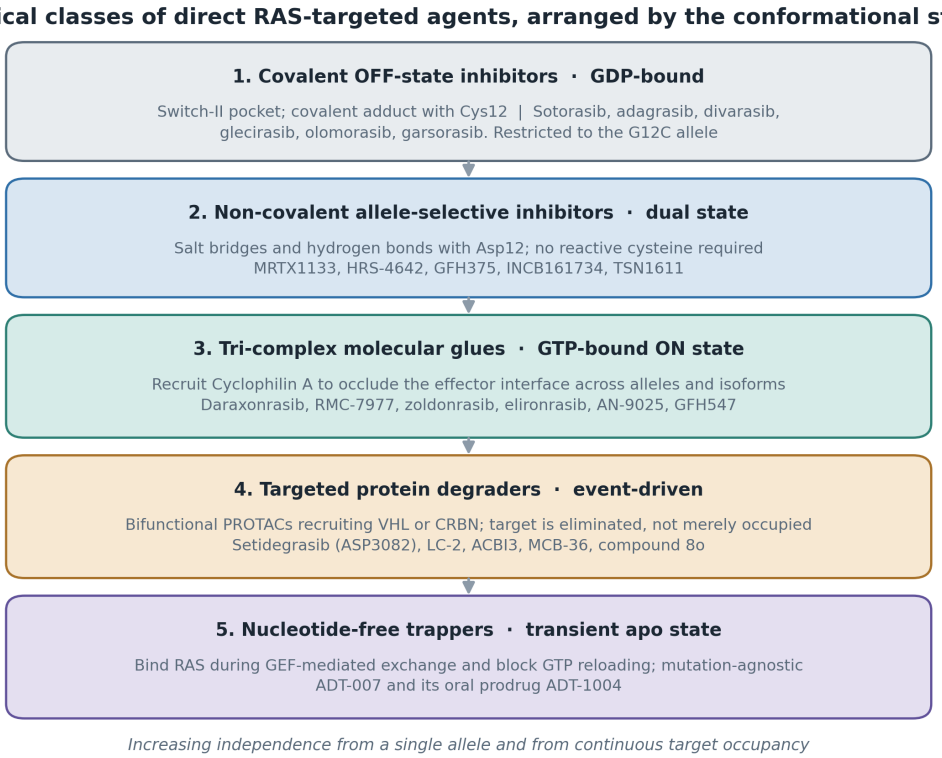


Figure 3. Five pharmacological classes of direct RAS-targeted agents, arranged by the conformational state each exploit. Classes are ordered from those requiring the inactive GDP-bound state at the top to those engaging transient or active species below, with representative agents named in each band. The arrangement makes the field's trajectory explicit: allele breadth and independence from continuous target occupancy both increase as agents move away from dependence on the inactive conformation and on a mutation-supplied covalent handle. Covalent OFF-state chemistry remains restricted to KRAS G12C, whereas tri-complex glues, degraders and nucleotide-free trappers reach the G12D, G12V and G12R alleles that predominate in pancreatic and colorectal cancer. Detailed mechanisms for each agent appear in Table 1.

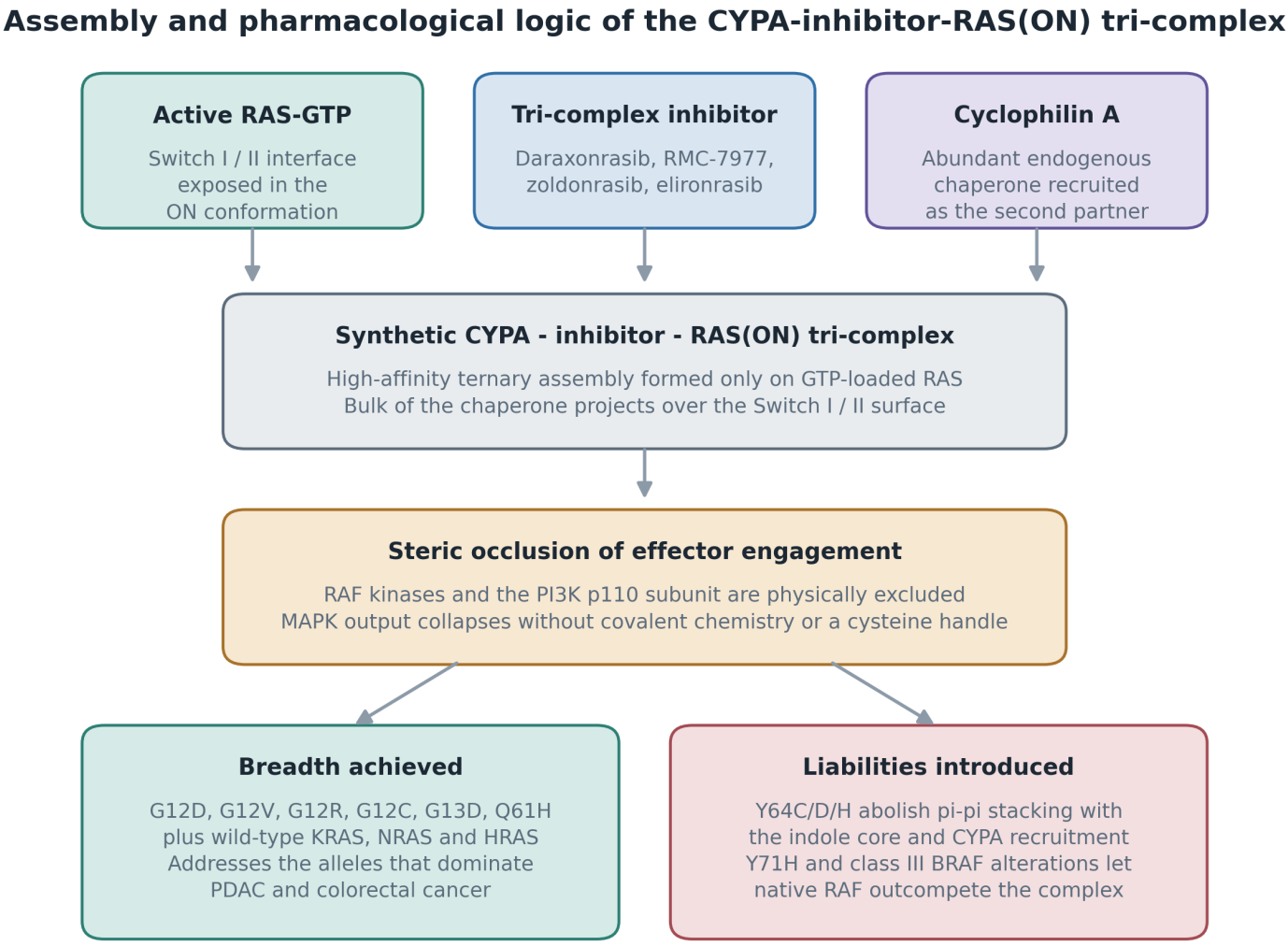


Figure 4. Assembly and pharmacological logic of the cyclophilin A-inhibitor-RAS(ON) tri-complex. Three components converge: active GTP-loaded RAS presenting an exposed Switch I/II interface, the tri-complex inhibitor, and the abundant endogenous chaperone cyclophilin A recruited as an obligate second partner. The resulting high-affinity ternary assembly forms only on GTP-bound protein, and the bulk of the chaperone projects across the switch surface so that RAF kinases and the PI3K p110 subunit are physically excluded without the drug occupying the effector site or reacting with a cysteine. The lower panels contrast what this buys, namely coverage of G12D, G12V, G12R, G12C, G13D and Q61H alongside wild-type isoforms, against the liabilities it introduces at the Y64, Y71 and BRAF nodes detailed in Table 3.

from occupancy to event: a bifunctional molecule brings an E3 ubiquitin ligase into proximity with the target, the ternary complex supports polyubiquitination, and the proteasome does the rest (L. Jiang et al., 2025). The catalytic nature of this mechanism means sustained target coverage is not required, which in principle blunts the resistance that arises from competitive displacement or copy-number gain.

The early history illustrates how much depends on cell biology rather than chemistry. CRBN-based covalent degraders such as XY-4-88 degraded overexpressed GFP-tagged KRAS G12C but failed against endogenous protein, apparently because cytoplasmic CRBN and membrane-anchored KRAS do not co-localise sufficiently (Bond et al., 2020). Switching to VHL recruitment solved this: LC-2, built on an adagrasib warhead, degraded endogenous KRAS G12C with DC50 values of 0.25 to 0.76 micromolar and suppressed downstream ERK signalling (Bond et al., 2020). For G12D, setidegrasib (ASP3082) recruits VHL selectively and, in quantitative proteomic profiling across more than 9,000 proteins, degraded mutant KRAS without touching the wild-type protein (Yoshinari et al., 2025). Compound 8o, derived by linking MRTX1133 to a VHL ligand, achieved DC50 of 38.1 nM with antiproliferative IC50 values of 31 to 60 nM in G12D PDAC models (Zhou et al., 2024). Pan-KRAS degraders such as ACBI3 bind GDP-loaded variants with roughly picomolar affinity and induced complete regression in xenografts carrying G12D, G12V, or G13D without evident systemic toxicity (Popow et al., 2024). Indirect degradation of SOS1, FAK, and AKT offers a complementary route to suppressing adaptive signalling (L. Jiang et al., 2025).

2.5.2. Trapping the nucleotide-free intermediate

A fourth state deserves attention, and it is the one that exists only fleetingly. During GEF-mediated exchange, RAS passes through a nucleotide-free apo intermediate, and ADT-007 with its oral prodrug ADT-1004 bind selectively to that species, blocking GTP reloading (Bandi et al., 2025). Because exchange is obligatory for both mutant and wild-type cycling, the activity is mutation-agnostic, and ADT-1004 produced regressions in PDAC models resistant to sotorasib, adagrasib, and MRTX1133 (Bandi et al., 2025).

The selectivity mechanism is unusual enough to be worth spelling out. Normal tissues express UDP-glucuronosyltransferases that glucuronidate the phenolic hydroxyl required for RAS binding, inactivating the compound; KRAS-mutant tumour cells express little UGT, so active drug accumulates preferentially there (Bandi et al., 2025). This is metabolic rather than molecular selectivity, which makes it elegant but also dependent on a tumour property that may vary between patients more than a mutation does. ADT-1004 additionally increased M1 macrophage polarisation, dendritic cell activation, and cytotoxic T-cell infiltration (Bandi et al., 2025). The data remain preclinical.

2.6. Resistance architecture and the logic of combination

Every modality described above has met resistance, and the mechanisms differ enough between modalities to be diagnostically useful (Isermann et al., 2025; Sang et al., 2026). For OFF-state covalent inhibitors the dominant on-target lesions are Switch-II pocket substitutions: Y96C confers cross-resistance to both sotorasib and adagrasib, whereas H95D/Q/R impairs adagrasib binding while sparing sotorasib, a distinction with immediate sequencing implications (Awad et al., 2021; Tanaka et al., 2021; Zhao et al., 2021).

Tri-complex inhibitors fail differently, and the structural basis is now reasonably well defined. Tyrosine 64 makes a pi-pi stacking contact with the indole core of daraxonrasib; Y64C, Y64D, and Y64H abolish it, raising the concentration required for complex formation roughly twenty-fold and impairing cyclophilin A recruitment (Sang et al., 2026). A second archetype does not touch the drug interface at all. Y71H introduces a neomorphic contact with Arg67 of the CRAF Ras-binding domain, increasing RAS-RAF affinity so that native effector simply outcompetes the synthetic complex (Sang et al., 2026). Class III hypoactive BRAF alterations achieve a similar end by promoting dimerisation and repositioning the cysteine-rich domain (Sang et al., 2026). Focal KRAS amplification, found in 62% of acquired resistance cases in one cell-free DNA series, works by a cruder route, simply outnumbering the drug (Aronchik et al., 2025; Sang et al., 2026). Next-generation tri-complex agents such as RMC-4791 adopt an altered binding geometry that tolerates Y64 substitution (Sang et al., 2026), and pharmacological restoration of GTP hydrolysis offers a conceptually different escape from this trap (Cuevas-Navarro et al., 2025).

Non-genetic resistance may ultimately prove harder. Inhibition of RAS-MAPK signalling mislocalises the polarity protein Scribble, permitting YAP/TAZ nuclear translocation and TEAD-dependent transcription, which amplifies MYC and upregulates MRAS to establish a RAS-independent survival programme (Adachi et al., 2023; Wasko et al., 2024). EMT and lineage switching operate along similar lines (Adachi et al., 2020; Singhal et al., 2024). These states are reversible and epigenetically encoded, so they are not detectable by mutation calling, which is a real limitation for ctDNA-based monitoring.

The combination frameworks now in trials map onto these archetypes fairly directly (Figure 5; Table 4). Vertical blockade pairs RAS-directed agents with SHP2 or SOS1 inhibitors to close the exchange loop (Daley et al., 2025; Kang et al., 2025; Zhong et al., 2025). In colorectal cancer, where EGFR feedback is rapid and near-universal, anti-EGFR antibody combination has already become standard practice (Fakih et al., 2023; Yaeger et al., 2023). Bypass signalling is addressed with allosteric TEAD inhibitors (Edwards et al., 2023; Hagenbeek et al., 2023). Immuno-oncology integration exploits the microenvironmental remodelling that RAS inhibition itself produces (Broderick et al., 2025; Orlen et al., 2025; Patel et al., 2025). Synthetic lethality in MTAP-deleted tumours supports PRMT5 inhibitor pairing (Drizyte-Miller et al., 2025; Pant et al., 2026), and treatment-induced CLDN18.2 upregulation offers a route to antibody-drug conjugates and cell therapy (Habib et al., 2026). Serial ctDNA monitoring underpins all of this by making resistance visible before radiographic progression (Chan et al., 2026).

3. Methods

3.1. Design and reporting framework

This is a structured narrative review of allosteric and state-selective pharmacology directed at RAS. We considered and rejected a formal meta-analysis, and the reason is worth stating rather than glossing: the evidence base spans crystallographic and biophysical characterisation, preclinical efficacy in heterogeneous model systems, single-arm early phase cohorts of fewer than fifty patients, and one randomised Phase III trial. Pooling response rates across such different designs would generate a number with the appearance of precision and very little meaning. Evidence was instead identified systematically and synthesised narratively, with the procedure documented in enough detail to be repeated (Figure 1). Reporting follows PRISMA 2020 items applicable to narrative synthesis. No protocol was registered, which we note as a limitation.

3.2. Information sources and search strategy

We searched PubMed/MEDLINE, Embase, Scopus, and Web of Science Core Collection, together with ClinicalTrials.gov for trial status and enrolment figures and the abstract archives of AACR, ASCO, and ESMO for data not yet in full publication. The window ran from 1 January 2013, the year the Switch-II pocket was described, to 31 May 2026. Searches were restricted to English-language records. Because several agents discussed here have changed names between development codes and international non-proprietary names, both forms were searched for each compound.

The PubMed strategy combined MeSH headings with free-text terms and was translated into the syntax of the other databases without altering its logic. The executable string was: ("Proto-Oncogene Proteins p21(ras)"[MeSH Terms] OR KRAS[tiab] OR NRAS[tiab] OR HRAS[tiab] OR "RAS GTPase"[tiab]) AND (allosteric[tiab] OR "switch II"[tiab] OR "molecular glue"[tiab] OR "tri-complex"[tiab] OR "cyclophilin A"[tiab] OR PROTAC[tiab] OR "targeted protein degradation"[tiab] OR "nucleotide-free"[tiab] OR degrader[tiab]) AND (sotorasib[tiab] OR adagrasib[tiab] OR MRTX1133[tiab] OR daraxonrasib[tiab] OR RMC-6236[tiab] OR zoldonrasib[tiab] OR ASP3082[tiab] OR "drug resistance, neoplasm"[MeSH Terms] OR "clinical trial"[Publication Type]). Reference lists of all included full texts were hand-searched and forward citation checking was performed for the structural and Phase III reports.

3.3. Eligibility criteria

Records were eligible if they reported structural or biophysical characterisation of a RAS-directed agent and its binding site; preclinical efficacy with quantitative potency, degradation, or regression data; clinical evaluation of a direct RAS-targeted agent at any phase; or genomic, structural, or functional characterisation of resistance to such agents. We excluded reports addressing only downstream pathway inhibition without a direct RAS-binding component, studies of RAS biology without pharmacological application, and editorials or commentaries. Conference abstracts were retained where they represented the only available source for a clinical dataset, and are identified as such wherever cited, since

their data are provisional and have not been peer reviewed in full.

3.4. Selection and data extraction

Records were deduplicated, screened by title and abstract, and assessed in full text. Two reviewers worked independently at each stage, with disagreements resolved by discussion and a third reviewer adjudicating where consensus failed. Data were extracted into a standardised template capturing: agent name and development code; chemical modality; target allele and isoform coverage; nucleotide conformation engaged; binding pocket and principal molecular interactions; potency metrics reported as IC50, KD, DC50, or Dmax with the assay system specified; model system and species for preclinical data; trial identifier, phase, line of therapy, and sample size; objective response rate, disease control rate, median progression-free and overall survival; ctDNA dynamics where reported; grade 3 or higher treatment-related adverse event rates; and resistance alterations with their detection method.

3.5. Handling of heterogeneous efficacy data

Comparability was the principal methodological difficulty, and we handled it conservatively. Potency values are reproduced exactly as reported, with units and assay context preserved, because binding affinities measured by surface plasmon resonance, isothermal titration calorimetry, and cellular target engagement assays are not interchangeable. Clinical outcomes are reported by line of therapy and tumour type and are never pooled across trials; where two agents are discussed in sequence, no statistical comparison between them is implied, since the cohorts differ in size, prior therapy, and allele distribution. Randomised evidence is identified explicitly wherever it exists, and single-arm data are labelled as such. Where a dataset exists only as a conference abstract, we say so at the point of citation.

3.6. Quality appraisal and synthesis

Preclinical studies were appraised on whether the model system was defined by allele and species, whether immunocompetent models were used for immunological claims, whether appropriate wild-type controls were included, and whether pharmacokinetic exposure was reported alongside efficacy. Clinical studies were appraised on design, sample size, blinding where applicable, completeness of safety reporting, and whether response assessment used standard criteria. Findings were then organised into four evidence domains corresponding to (Table 1) through (Table 4) and synthesised narratively, with attention to distinguishing results replicated independently from those resting on a single group or a single cohort.

4. Synthesis of Findings: What the Evidence Now Supports Across Four Domains

4.1. Structural classes and the conformational states they exploit

Read across the structural and biochemical literature, direct RAS-targeted agents resolve into five mechanistic classes, and the organising variable is which conformational state each requires (Alanazi et al., 2025; Chan et al., 2026). (Figure 3) arranges them on that axis; (Table 1) gives the detail.

The foundational class remains the covalent OFF-state inhibitors. Sotorasib and adagrasib modify Cys12 within the Switch-II pocket of GDP-bound KRAS G12C, locking the protein out of the exchange cycle and preventing RAF/MEK/ERK engagement (Canon et al., 2019; Ostrem et al., 2013; Skoulidis et al., 2021). Their dependence on a reactive cysteine is absolute, which is what confines them to one allele (Isermann et al., 2025).

Non-covalent allele-selective agents relaxed that constraint. MRTX1133 achieves sub-picomolar affinity for KRAS G12D through salt bridges with the mutant aspartate and can engage both GDP- and GTP-bound states, stabilising Switch II while leaving Switch I dynamically uncoupled from effector engagement (Hallin et al., 2022; X. Wang et al., 2022). In immunocompetent PDAC models it produced regression together with substantial microenvironmental change, repolarising macrophages, depleting MDSCs, and increasing CD8+ infiltration (Hallin et al., 2022).Tri-complex molecular glues represent the largest conceptual step. Daraxonrasib and RMC-7977 bind the GTP-bound Switch I/II interface and recruit cyclophilin A into a high-affinity synthetic ternary complex that sterically excludes RAF and PI3K (Cregg et al., 2025; Holderfield et al., 2024; Schulze et al., 2023). The resulting coverage spans G12D, G12V, G12R, G12C, G13D, and Q61H as well as wild-type KRAS, NRAS, and HRAS (Holderfield et al., 2024). Covalent variants such as zoldonrasib apply the same architecture to active G12D specifically, bonding to

Table 1. Structural classes, conformational states and biochemical mechanisms of direct RAS-targeted inhibitors and degraders. This table sets out the principal direct RAS-targeted agents according to the chemical modality they employ, the allele and nucleotide conformation each engages, the structural pocket and molecular interactions responsible for binding, and the cellular and microenvironmental consequences that follow. Entries are ordered to follow the historical progression from allele-restricted covalent chemistry through non-covalent and active-state approaches to event-driven degradation and apo-state trapping. Reading down the conformational-state column makes the central argument of this review visible: breadth of allele coverage tracks with independence from the inactive state rather than with binding potency.

Agent and class	Allele and conformational state	Binding pocket and interaction	Biochemical mechanism	Cellular and microenvironmental effect	Key references
Sotorasib (AMG 510) Covalent OFF-state inhibitor	KRAS G12C; inactive GDP-bound state	Cryptic Switch-II pocket beneath the Switch II loop; irreversible covalent adduct with Cys12	Traps KRAS G12C in the GDP conformation, preventing nucleotide exchange and blocking RAF/MEK/ERK engagement	Suppresses pERK; promotes pro-inflammatory microenvironmental remodelling with increased CD8+ T-cell infiltration and synergy with anti-PD-1	Canon et al. (2019); Ostrem et al. (2013); Skoulidis et al. (2021)
Adagrasib (MRTX849) Covalent OFF-state inhibitor	KRAS G12C; inactive GDP-bound state	Switch-II pocket; covalent bond to Cys12 with extensive hydrophobic contacts	Irreversibly locks the mutant protein in the GDP state; long half-life and high tissue accumulation with central nervous system penetration	Tumour regression across NSCLC, CRC and PDAC; documented intracranial activity in brain metastases	Jänne et al. (2022); Ostrem et al. (2013)
MRTX1133 Non-covalent allele-selective inhibitor	KRAS G12D; engages both inactive and active states	Switch-II pocket; salt bridges and hydrogen-bond network with Asp12 without covalent attachment	Sub-picomolar binding (KD approximately 0.2 pM) stabilising an inactive-like conformation; disrupts effector engagement without a reactive cysteine	Deep regression in G12D PDAC models; repolarises M2 macrophages toward M1, depletes MDSCs and reprogrammes cancer-associated fibroblasts	Hallin et al. (2022); X. Wang et al. (2022)
Daraxonrasib (RMC-6236) Tri-complex molecular glue	Pan-RAS, multi-selective; active GTP-bound state	Active Switch I/II interface; recruits cyclophilin A as an obligate second partner	Forms a synthetic CYPA-inhibitor-RAS(ON) tri-complex that sterically occludes RAF and PI3K binding across G12D, G12V, G12R, G12C and wild-type RAS	Complete MAPK silencing across diverse alleles; overcomes upstream RTK feedback that defeats OFF-state agents	Cregg et al. (2025); Holderfield et al. (2024); Schulze et al. (2023)
RMC-7977 Tri-complex molecular glue (tool compound)	Pan-RAS; active GTP-bound state	Active Switch I/II interface with cyclophilin A recruitment	Concurrent inhibition of oncogenic and wild-type RAS-GTP, establishing the tolerability of pan-RAS suppression in vivo	Marked regression and microenvironmental remodelling in immunocompetent models across KRAS G12X variants	Holderfield et al. (2024); Wasko et al. (2024)
Zoldonrasib (RMC-9805) Covalent active-state tri-complex inhibitor	KRAS G12D; active GTP-bound state	Active Switch II pocket; covalent handle to Asp12 with cyclophilin A recruitment	Covalently engages active GTP-loaded KRAS G12D while assembling the chaperone complex, blocking effector access selectively	Rapid ctDNA clearance with selective target engagement and no wild-type RAS toxicity in normal tissue	Schulze et al. (2023); Spira et al. (2025)
Setidegrasib (ASP3082) Targeted protein degrader (PROTAC)	KRAS G12D; mutant-selective degradation	G12D-directed warhead linked to a VHL E3 ubiquitin ligase ligand	Ternary KRAS G12D-degrader-VHL complex drives polyubiquitination and 26S proteasomal destruction of the mutant protein	Selective clearance of KRAS G12D across more than 9,000 quantified proteins; complete tumour regression and deep ctDNA responses	Park et al. (2026); Yoshinari et al. (2025)

Compound 8o VHL-based degradation compound	KRAS G12D; selective degradation	Optimised MRTX1133 warhead with 7-fluoronaphthyl modification linked to a VHL ligand	Potent selective degradation (DC50 38.06 nM) with pERK suppression sustained beyond 24 hours in AsPC-1 PDAC cells	Dose-dependent growth arrest (IC50 31–60 nM) and complete xenograft regression without weight loss	Zhou et al. (2024)
ACBI3 and pan-KRAS degraders Targeted protein degrader	Pan-KRAS variants; GDP-bound state	Pan-KRAS binder linked to an E3 ligase ligand; picomolar affinity for GDP-loaded protein	Induces degradation across multiple mutant variants rather than a single allele	Complete regression in xenografts harbouring G12D, G12V or G13D without evident systemic toxicity	Popow et al. (2024)
LC-2 VHL-recruiting PROTAC	KRAS G12C; covalent warhead	Adagrasib-derived warhead linked to a VHL ligand	Rapid and sustained degradation of endogenous KRAS G12C (DC50 0.25–0.76 μM) after earlier CRBN-based degraders failed on endogenous protein	Downstream ERK inhibition; established that E3 ligase choice and subcellular localisation govern degrader success	Bond et al. (2020)
ADT-007 and ADT-1004 Nucleotide-free trapper	Pan-RAS; transient apo (nucleotide-free) state	Binds the nucleotide-free intermediate formed during GEF-mediated exchange	Traps apo-RAS and prevents GTP reloading across mutant and wild-type isoforms; tumour selectivity arises from low UGT expression in tumour cells	Overcomes resistance to G12C and G12D monotherapies; increases M1 polarisation, dendritic cell activation and CD8+ infiltration	Bandi et al. (2025)

Table 2. Clinical trial landscape, efficacy metrics and safety profiles of direct RAS-targeted agents in pancreatic and other solid tumours. This table assembles the clinical evidence for direct RAS-targeted therapy, giving for each programme the trial phase and setting, the biomarker-defined population, sample size, response and disease-control rates, survival outcomes, and the toxicities that define its tolerability. Trials are listed in approximate order of development maturity. Readers should note that all but two entries are single-arm cohorts of fewer than sixty patients, so figures are not comparable across rows and no cross-trial inference is intended; only RASolute-302 and CodeBreaK 300 provide randomised comparison. Entries drawn from conference abstracts are identified in the final column.

Agent and trial	**Phase and setting**	**Population**	**n**	**ORR and DCR**	**PFS and OS**	**Safety**	**Clinical interpretation and reference**
Sotorasib (CodeBreaK 100)	Phase I/II, single arm	Pretreated KRAS G12C PDAC	38	ORR 21.1%; DCR 84.2%	mPFS 4.0 months; mOS 6.9 months	Diarrhoea (20%), transaminase elevation; grade 3 TRAEs 15.8%	First proof of concept for direct KRAS inhibition in PDAC (Strickler et al., 2023)
Adagrasib (KRYSTAL-1)	Phase I/II, single arm	Pretreated KRAS G12C PDAC	21	ORR 33.3%; DCR 81.0%	mPFS 5.4 months; mOS 8.0 months	Nausea, vomiting, diarrhoea, QTc prolongation; grade 3 TRAEs 24%	Confirms G12C targetability in gastrointestinal malignancy (Bekaii-Saab et al., 2023)
Glecirasib (JAB-21822), pooled analysis	Phase I/II, pooled GI cohort	Pretreated KRAS G12C pancreatic cancer	32	ORR 46.9%; DCR 93.8%	mPFS 5.5 months; mOS 10.8 months	Anaemia, transaminase elevation, rash; low discontinuation rate	Highest monotherapy activity reported within the G12C class; conference abstract (Li et al., 2024)

Daraxonrasib (RASolute-302)	Phase III, randomised versus chemotherapy	Pretreated RAS-mutant metastatic PDAC	228	Significantly superior to chemotherapy	mOS 13.2 vs 6.7 months (HR 0.40); mPFS 7.3 vs 3.5 months (HR 0.49), both $p < 0.001$	Rash, stomatitis, diarrhoea; grade 3 TRAEs 43.6% versus 57.5% with chemotherapy	Practice-changing randomised evidence for pan-RAS inhibition (O'Reilly et al., 2026)
Daraxonrasib plus gemcitabine/nab-paclitaxel (RMC-GI-102)	Phase I/Ib	Treatment-naive RAS-mutant metastatic PDAC	30	ORR 58–59%; DCR 97%	6-month PFS 84%; mOS not reached	Neutropenia, rash, fatigue; expected chemotherapy toxicities	Supports first-line combination of a pan-RAS(ON) agent with chemotherapy; conference abstract (Wolpin et al., 2026)
Zoldonrasib monotherapy	Phase I, first in human	Pretreated KRAS G12D PDAC	40	ORR 30%; DCR 80%	Not mature at reporting	Generally low-grade; selective for mutant protein	86% of evaluable patients achieved >50% ctDNA reduction and 39% cleared ctDNA; conference abstract (Spira et al., 2025)
Zoldonrasib plus daraxonrasib (RMC-9805-001)	Phase I/Ib	Pretreated KRAS G12D metastatic PDAC, second and third line	60	2L ORR 50% (DCR 97%); 3L+ ORR 47% (DCR 90%)	2L mPFS 9.6 months; 3L+ mPFS 7.6 months, mOS 10.5 months	Grade 3 TRAEs 35%; low discontinuation rate	Dual ON-state targeting yields deep, durable responses; conference abstract (Azad et al., 2026)
Setidegrasib (ASP3082)	Phase I, 600 mg RP2D cohort	Advanced KRAS G12D PDAC	21	ORR 24%; DCR 85.7%	mPFS 3.0 months; mOS 10.3 months	Infusion-related reactions 80% (grade 1–2); grade 3 TRAEs 9%	Clinical validation of targeted protein degradation in mutant KRAS PDAC (Park et al., 2026)
HRS-4642 plus gemcitabine/nab-paclitaxel	Phase Ib/II combination	Treatment-naive KRAS G12D advanced PDAC	30	ORR 60.0%; DCR 93.3%	17 of 18 responses ongoing at 4.4 months of follow-up	Myelosuppression, peripheral neuropathy, fatigue	High activity for a dual-state non-covalent G12D inhibitor with chemotherapy (L. Wang et al., 2025)
Sotorasib plus panitumumab (CodeBreaK 300)	Phase III, randomised	Pretreated KRAS G12C metastatic CRC	160	ORR 26.4% versus 0% with chemotherapy	mPFS 5.6 vs 2.2 months ($p = 0.005$)	Rash, hypomagnesaemia, fatigue	Randomised confirmation that EGFR co-inhibition is required in CRC (Fakih et al., 2023

Asp12 while recruiting the chaperone, which preserves selectivity against wild-type protein in normal tissue (Schulze et al., 2023; Spira et al., 2025). The assembly is depicted in (Figure 4).

Targeted degradation substitutes elimination for occupancy. Setidegrasib recruits VHL to KRAS G12D, and quantitative proteomics across more than 9,000 proteins showed degradation confined to the mutant species, with complete regressions in PDAC models (Park et al., 2024, 2026; Yoshinari et al., 2025). Compound 8o, built from an MRTX1133 warhead, achieved DC50 of 38.06 nM with pERK suppression sustained beyond 24 hours in AsPC-1 cells (Zhou et al., 2024), and pan-KRAS degraders extend the approach across variants (Popow et al., 2024). Finally, nucleotide-free trappers intercept the apo intermediate during GEF-mediated exchange; ADT-1004 blocks GTP reloading on mutant and wild-type protein alike and achieves tumour selectivity through differential UGT-mediated inactivation in normal tissue (Bandi et al., 2025).

4.2. Clinical efficacy and safety across PDAC and other solid tumours

The clinical record shows a fairly clear gradient, though it should be read with the caveat that most of these are single-arm cohorts of modest size (Table 2). First-generation G12C inhibitors established proof of concept in the 1% to 2% of PDAC carrying that allele. In CodeBreaK 100, sotorasib produced an ORR of 21.1% with disease control in 84.2%, median PFS of 4.0 months and median OS of 6.9 months in 38 patients (Strickler et al., 2023). KRYSTAL-1 gave broadly similar results for adagrasib in 21 patients: ORR 33.3%, DCR 81.0%, median PFS 5.4 months, median OS 8.0 months (Bekaii-Saab et al., 2023). A pooled analysis of glecirasib in 32 pretreated patients reported a confirmed ORR of 46.9% with median OS of 10.8 months (Li et al., 2024), which suggests genuine improvement within the class, though cross-trial comparison at these sample sizes is not reliable.

For G12D, the dominant PDAC allele, active-state and degrader approaches have both produced early signals. Zoldonrasib monotherapy in 40 pretreated patients achieved an ORR of 30% and DCR of 80%; among 28 with detectable baseline ctDNA, 86% showed a reduction greater than 50% and 39% cleared entirely (Spira et al., 2025). Setidegrasib at its recommended Phase II dose of 600 mg gave an ORR of 24%, median PFS of 3.0 months, median OS of 10.3 months, and a median ctDNA reduction of 91.3% in 21 patients, with grade 3 or higher events in 9% and largely low-grade infusion reactions in 80% (Park et al., 2026). In treatment-naive G12D disease, HRS-4642 with gemcitabine and nab-paclitaxel reported a confirmed ORR of 60% and DCR of 93.3% (L. Wang et al., 2025).

The pivotal evidence comes from RASolute-302, which randomised previously treated patients with RAS-mutant metastatic PDAC to oral daraxonrasib or investigator's choice chemotherapy (O'Reilly et al., 2026). Daraxonrasib improved median overall survival from 6.7 to 13.2 months (HR 0.40) and median progression-free survival from 3.5 to 7.3 months (HR 0.49), both at $p < 0.001$ (Chan et al., 2026; O'Reilly et al., 2026). Grade 3 or higher treatment-related events occurred in 43.6% of daraxonrasib recipients versus 57.5% on chemotherapy, with rash and stomatitis predominating and manageable by dose modification (Ahmed et al., 2026; O'Reilly et al., 2026). A doubling of median survival in second-line metastatic pancreatic cancer is not a marginal result, and it is the first randomised demonstration that pan-RAS inhibition is both feasible and tolerable.

Combination data are following. Daraxonrasib with gemcitabine and nab-paclitaxel in treatment-naive RAS-mutant PDAC produced an ORR of 58% to 59%, DCR of 97%, and a six-month PFS rate of 84% (Wolpin et al., 2026). Pairing zoldonrasib with daraxonrasib gave an ORR of 50% with median PFS of 9.6 months in second line, and 47% with median OS of 10.5 months in third line or later (Azad et al., 2026). These remain early-phase findings awaiting randomised confirmation.

4.3. The molecular architecture of resistance

Genomic profiling of post-progression tissue and cell-free DNA shows resistance arising through four broad routes, and they differ by modality in ways that are mechanistically coherent (Table 3; Figure 5). For covalent OFF-state inhibitors, secondary Switch-II pocket substitutions dominate: Y96C, H95D/Q/R, R68S, and Q99L disrupt drug docking while leaving nucleotide cycling intact (Awad et al., 2021; Isermann et al., 2025; Tanaka et al., 2021). The pattern is drug-specific in a clinically useful way, since Y96C compromises both sotorasib and adagrasib while H95D/Q/R impairs adagrasib but spares sotorasib (Isermann et al., 2025; Zhao et al., 2021).

Tri-complex inhibitors encounter a different set. Structural and CRISPR base-editing screens identified KRAS Y64C,

Table 3. Molecular, structural and cellular mechanisms of resistance to inactive-state and active-state RAS-targeted agents. This table organises resistance by node rather than by drug, specifying for each category the alterations observed, the inhibitor classes affected, the structural or biochemical basis of escape, and the downstream signalling consequence. The arrangement is intended to be diagnostically useful: on-target pocket mutations, glue-interface disruption, effector-level competition, copy-number gain and non-genetic bypass each point toward a different combinatorial response, as mapped in Figure 5 and Table 4. Note that the final two categories are not detectable by mutation calling, which limits what serial circulating tumour DNA monitoring can be expected to identify.

Resistance node	Alterations observed	Inhibitor classes affected	Structural or biochemical mechanism	Signalling consequence	Key references
On-target Switch-II pocket mutation	KRAS Y96C, H95D/Q/R, R68S, Q99L	Covalent OFF-state G12C inhibitors (sotorasib, adagrasib)	Disrupts steric docking, hydrogen bonding or covalent adduct formation within the Switch-II pocket while leaving nucleotide cycling intact	Restores GTP loading and RAF/MEK/ERK output despite continued drug exposure; Y96C affects both agents whereas H95D/Q/R spares sotorasib	Awad et al. (2021); Tanaka et al. (2021); Zhao et al. (2021)
Tri-complex glue interface disruption	KRAS Y64C, Y64D, Y64H	Multi-selective RAS(ON) tri-complex inhibitors (daraxonrasib)	Removes the aromatic ring required for pi-pi stacking with the inhibitor indole core, raising the EC50 for complex formation roughly twenty-fold and weakening cyclophilin A recruitment	Prevents assembly of the synthetic CYPA-inhibitor-RAS complex, allowing native RAF to bind active RAS	Cuevas-Navarro et al. (2025); Sang et al. (2026)
Neomorphic RAS-RAF affinity enhancement	KRAS Y71H	Multi-selective RAS(ON) tri-complex inhibitors	Introduces a neomorphic electrostatic and pi-cation contact with Arg67 of the CRAF Ras-binding domain without touching the drug interface	Native RAF outcompetes the inhibitor-chaperone complex; binder optimisation cannot address this route	Sang et al. (2026)
RAF dimerisation and hypoactive alterations	BRAF D594A/G/N, G466E/A, K483E (class III)	Multi-selective RAS(ON) tri-complex inhibitors	Constitutive RAF dimerisation repositions the cysteine-rich domain to maximise KRAS binding	RAF becomes resistant to displacement by the tri-complex, sustaining ERK activity	Sang et al. (2026)
Oncogenic gene amplification	Focal KRAS amplification (62% of acquired resistance cases in cell-free DNA)	Both OFF-state and ON-state inhibitors	Increases oncogenic protein abundance beyond the coverage achievable at tolerated drug exposure	Restores net pathway output by overwhelming competitive inhibition	Aronchik et al. (2025); Sang et al. (2026)
Upstream RTK and exchange-factor feedback	HGF-MET autocrine loop; EGFR/HER2/HER3 upregulation; SOS1 and SHP2 hyperactivation	OFF-state covalent and non-covalent allele-specific inhibitors	Loss of negative MAPK feedback reactivates upstream receptors, driving SOS1- and SHP2-mediated GTP loading on wild-type NRAS/HRAS or newly synthesised KRAS	Rapidly restores active GTP-bound RAS, bypassing agents that depend on the inactive state	Isermann et al. (2025); Singhal et al. (2024)
Hippo-YAP/TAZ transcriptional bypass	Scribble mislocalisation, nuclear YAP/TAZ translocation, TEAD activation, MYC amplification	Pan-RAS(ON) inhibitors and broad-spectrum agents	Disrupted membrane localisation of Scribble permits YAP/TAZ nuclear entry and TEAD-dependent transcription of MYC and MRAS	Establishes an orthogonal, RAS-independent survival and proliferation programme	Adachi et al. (2023); Edwards et al. (2023); Wasko et al. (2024)
Phenotypic plasticity and lineage switching	Epithelial-mesenchymal transition; ZEB1 and TWIST upregulation	Broad-spectrum RAS inhibitors and degraders	Epigenetic reprogramming causes loss of epithelial identity and downregulation of epithelial driver dependencies	Shifts cells toward an invasive, stem-like phenotype with reduced canonical MAPK dependence	Adachi et al. (2020); Singhal et al. (2024)

Y64D, and Y64H as the principal on-target lesions; tyrosine 64 provides pi-pi stacking with the indole core of daraxonrasib, and its substitution raises the EC50 for tri-complex formation roughly twenty-fold while impairing cyclophilin A recruitment and preventing displacement of the RAF Ras-binding domain (Sang et al., 2026). The second archetype is more interesting because it does not involve the drug interface at all: Y71H introduces a neomorphic electrostatic contact with Arg67 of the CRAF RBD, raising RAS-RAF affinity so that native effector outcompetes the synthetic complex (Sang et al., 2026). Class III hypoactive BRAF alterations including G466A, G466E, D594A, and K483E reach the same endpoint through constitutive dimerisation and repositioning of the cysteine-rich domain (Sang et al., 2026). Longitudinal selection experiments showed Y64C emerging first, with BRAF G466A appearing subsequently and deepening resistance (Sang et al., 2026).

Copy-number gain works by a blunter mechanism. Focal KRAS amplification was identified in 62% of acquired resistance cases in cell-free DNA from daraxonrasib-treated patients, simply raising target abundance beyond what available drug can cover (Aronchik et al., 2025; Sang et al., 2026). Upstream feedback remains relevant across modalities, with HGF-MET autocrine loops, EGFR/HER2/HER3 upregulation, and SOS1/SHP2 hyperactivation restoring GTP loading on wild-type or newly synthesised protein (Isermann et al., 2025; Singhal et al., 2024).

Non-genetic adaptation completes the picture and is, we suspect, the most difficult of the four to address. Inhibition of RAS-MAPK signalling disrupts membrane localisation of Scribble, permitting YAP/TAZ nuclear translocation and TEAD-dependent transcription, which amplifies MYC and upregulates MRAS to establish a survival programme independent of RAS (Adachi et al., 2023; Wasko et al., 2024). Epithelial-mesenchymal transition with ZEB1 and TWIST upregulation shifts cells toward an invasive, stem-like phenotype with reduced MAPK dependence (Adachi et al., 2020; Singhal et al., 2024). Stromal contributions from cancer-associated fibroblasts sustain ERK phosphorylation independently of tumour-cell genotype (Chan et al., 2026). None of these is detectable by mutation calling, which limits what ctDNA surveillance can be expected to catch.

4.4. Biomarker-guided combination frameworks

Combination strategy now maps onto resistance archetype with reasonable directness (Table 4; Figure 5). The most mature example is anti-EGFR pairing in colorectal cancer, where feedback reactivation is rapid enough to blunt single-agent activity almost immediately. In the randomised Phase III CodeBreaK 300 trial, sotorasib with panitumumab improved median PFS to 5.6 months against 2.2 months for investigator's choice chemotherapy ($p = 0.005$) and raised ORR from 0% to 26.4% (Fakih et al., 2023). Adagrasib with cetuximab achieved an ORR of 34% and median OS of 15.9 months in pretreated G12C CRC (Yaeger et al., 2023).

Vertical blockade of the exchange machinery addresses the same feedback at a different node. SHP2 operates downstream of receptor tyrosine kinases to promote SOS1 recruitment and nucleotide exchange; combining the SHP2 inhibitor sitneprotafib with glecirasib produced durable responses in Phase I/II evaluation while delaying acquired resistance (Kang et al., 2025; Zhong et al., 2025), and SOS1 inhibition with BI-3406 blocks exchange on wild-type NRAS and HRAS during adagrasib or MRTX1133 treatment (Daley et al., 2025).Dual active-state targeting takes a different approach to polyclonal escape, pairing the allele-selective G12D(ON) agent zoldonrasib with multi-selective daraxonrasib so that both the primary mutant and wild-type isoforms are suppressed simultaneously (Azad et al., 2026; Chan et al., 2026). This combination is now in Phase III registrational evaluation. Immunological integration rests on the observation that RAS inhibition itself restores MHC class I expression, reduces PD-L1, depletes MDSCs, and increases CD8+ infiltration in immunocompetent models; combining pan-RAS(ON) agents with anti-PD-1 blockade produced durable immune-mediated control (Broderick et al., 2025; Orlen et al., 2025; Patel et al., 2025). For transcriptional bypass, allosteric TEAD inhibitors including IAG933, GNE-7883, and VT-104 disrupt YAP/TAZ binding, downregulate MYC, and restore sensitivity in resistant PDAC models (Edwards et al., 2023; Hagenbeek et al., 2023). Roughly 20% of PDAC tumours carry homozygous MTAP deletion, and the resulting MTA accumulation partially inhibits PRMT5, providing a synthetic-lethal opening for MTA-cooperative PRMT5 inhibitors combined with daraxonrasib (Drizyte-Miller et al., 2025; Pant et al., 2026). Finally, RAS pathway inhibition upregulates surface CLDN18.2, creating a rationale for sequential or concurrent CLDN18.2-directed antibody-drug conjugates

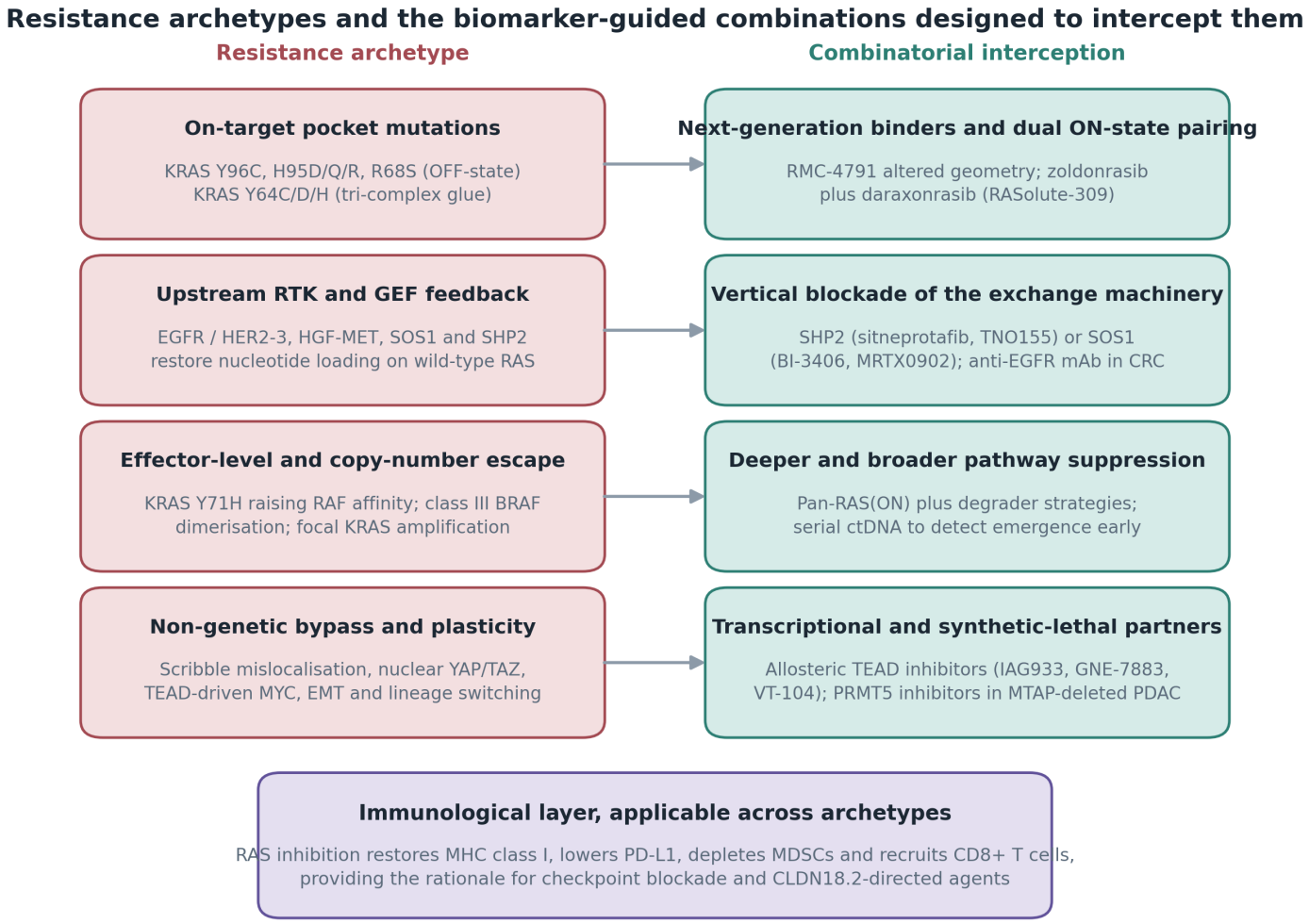


Figure 5. Resistance archetypes and the biomarker-guided combinations designed to intercept them. Each row pairs a mechanistically distinct route of escape, on the left, with the combinatorial strategy that addresses it, on the right. On-target pocket and glue-interface mutations are answered by next-generation binders and dual ON-state pairing; upstream receptor and exchange factor feedback by SHP2, SOS1 or anti-EGFR co-inhibition; effector-level competition and copy-number gain by deeper pathway suppression with serial ctDNA surveillance; and non-genetic bypass by transcriptional and synthetic-lethal partners. The panel at the foot indicates the immunological layer that applies across all four archetypes, since RAS inhibition itself remodels antigen presentation and the immune infiltrate. Corresponding trial evidence is tabulated in Table 4.

Table 4. Biomarker-guided combination strategies and multitargeted regimens for RAS-driven cancers. This table pairs each rational combination regimen with the resistance node it is designed to intercept, stating the mechanism of synergy, the current stage of clinical evaluation with representative trials, and the efficacy observed to date. It is intended to be read alongside Table 3, since each row answers a specific escape route rather than representing a general intensification of therapy. Stage of evidence varies widely across rows, from regulatory approval for EGFR co-inhibition in colorectal cancer to preclinical proof of concept for CLDN18.2-directed pairing, and the final column should be read with that gradient in mind.

Table 4. Biomarker-guided combination strategies and multitargeted regimens for RAS-driven cancers. This table pairs each rational combination regimen with the resistance node it is designed to intercept, stating the mechanism of synergy, the current stage of clinical evaluation with representative trials, and the efficacy observed to date. It is intended to be read alongside Table 3, since each row answers a specific escape route rather than representing a general intensification of therapy. Stage of evidence varies widely across rows, from regulatory approval for EGFR co-inhibition in colorectal cancer to preclinical proof of concept for CLDN18.2-directed pairing, and the final column should be read with that gradient in mind.

Combination	Target nodes	Mechanism of synergy	Stage and representative trial	Efficacy observed	Key references
G12C inhibitor plus anti-EGFR antibody	KRAS G12C and EGFR (sotorasib with panitumumab; adagrasib with cetuximab)	Blocks receptor-mediated adaptive feedback reactivation of wild-type RAS and MAPK signalling	Approved in CRC; Phase III CodeBreaK 300 and KRYSTAL-10	CodeBreaK 300: mPFS 5.6 vs 2.2 months (p = 0.005). KRYSTAL-1: ORR 34%, mOS 15.9 months in metastatic CRC	Fakih et al. (2023); Yaeger et al. (2023)
Dual active-state RAS(ON) combination	KRAS G12D plus multi-selective RAS(ON) (zoldonrasib with daraxonrasib)	Combines mutant-specific eradication with broad suppression of wild-type RAS and emerging secondary variants, reducing polyclonal rebound	Phase I/Ib RMC-9805-001; Phase III RASolute-309 active	Second line: ORR 50%, DCR 97%, mPFS 9.6 months. Third line or later: ORR 47%, mOS 10.5 months	Azad et al. (2026); O'Reilly et al. (2026)
RAS inhibitor plus SHP2 or SOS1 inhibitor	KRAS G12C or G12D with SHP2 or SOS1 (glecirasib with sitneprotafib; adagrasib with BI-3406)	Intercepts GEF-mediated nucleotide exchange and SOS1/SHP2 colocalisation, holding RAS in the inactive state	Phase I/II with Phase III planned	Manageable safety with improved ORR and PFS; delays emergence of acquired resistance	Daley et al. (2025); Kang et al. (2025); Zhong et al. (2025)
Pan-RAS(ON) agent plus immune checkpoint blockade	Pan-RAS(ON) with PD-1/PD-L1 (daraxonrasib or RMC-7977 with anti-PD-1)	RAS suppression restores MHC class I expression, lowers PD-L1, clears MDSCs and activates CD8+ T cells, converting an immunologically cold tumour	Preclinical with Phase III evaluation under way	Complete immune-mediated regression and sustained immune control in immunocompetent models	Broderick et al. (2025); Orlen et al. (2025); Patel et al. (2025)
Pan-RAS(ON) agent plus allosteric TEAD inhibitor	Pan-RAS(ON) with TEAD (RMC-7977 or daraxonrasib with IAG933, VT-104 or GNE-7883)	Blocks RAS-MAPK signalling while suppressing nuclear YAP/TAZ-TEAD-driven MYC transcription	Preclinical validation; Phase I evaluation	Downregulates MYC and reverses both intrinsic and acquired resistance in PDAC models	Edwards et al. (2023); Hagenbeek et al. (2023); Wasko et al. (2024)
Targeted agent plus cytotoxic chemotherapy	KRAS G12D or pan-RAS with gemcitabine/nab-paclitaxel or NALIRIFOX	Combines cytotoxic debulking with direct inhibition of driver signalling in the first-line setting	Phase Ib/II; Phase III RASolute-303	HRS-4642 with chemotherapy: first-line confirmed ORR 60.0%, DCR 93.3%. Daraxonrasib with chemotherapy: ORR 58–59%	L. Wang et al. (2025); Wolpin et al. (2026)
Pan-RAS(ON) agent plus PRMT5 inhibitor	Pan-RAS with PRMT5 in MTAP-deleted tumours (daraxonrasib with TNG462 or BMS-986504)	Exploits synthetic lethality in the approximately 20% of PDAC with homozygous MTAP deletion, where MTA accumulation already partially inhibits PRMT5	Phase I/II and Phase II/III	Synergistic tumour growth inhibition in MTAP-deleted, KRAS-mutant PDAC models	Drizyte-Miller et al. (2025); Pant et al. (2026)
RAS inhibitor plus CLDN18.2-directed agent	KRAS inhibitor with CLDN18.2 antibody-drug conjugate or CAR-T	Exploits drug-induced upregulation of surface CLDN18.2 following RAS pathway inhibition in PDAC	Preclinical proof of concept; Phase I trials active	Enhanced tumour cell killing and immune-mediated clearance in PDAC models	Habib et al. (2026); Singhal et al. (2024)

and CAR-T approaches (Habib et al., 2026).

5. What Changes When the Active State Becomes Druggable

5.1. The central shift, stated plainly

The most consequential development in this field is not any individual compound but a change in what the target is taken to be. For a decade after 2013, drugging RAS meant waiting for the protein to visit its inactive state and trapping it there, which imposed two requirements that turned out to be severely limiting: a reactive cysteine, and an allele that cycles often enough to make the inactive population accessible (Isermann et al., 2025; Ostrem et al., 2013). Tri-complex glues discarded both by treating the active conformation as the recognition element and recruiting a chaperone to do the blocking (Holderfield et al., 2024; Schulze et al., 2023). Degraders discarded the occupancy requirement altogether (L. Jiang et al., 2025), and apo-state trappers targeted a species that exists for milliseconds (Bandi et al., 2025). The comparison in (Figure 3) and (Table 1) is best read as a progression away from dependence on a particular mutation toward dependence on a state that all RAS-driven tumours must occupy.

The clinical validation of that shift is the RASolute-302 result: a doubling of median overall survival in second-line metastatic PDAC, a setting where incremental gains have been the norm for twenty years (O'Reilly et al., 2026). We would resist over-reading a single trial, and the follow-up is still maturing, but this is the strongest evidence yet that inhibiting wild-type alongside mutant RAS is survivable and therapeutically worthwhile.

5.2. The therapeutic window that theory did not predict

Pan-RAS inhibition should, on paper, be intolerable. Wild-type RAS is required in proliferating normal tissue, and an agent that suppresses it across isoforms might reasonably be expected to produce dose-limiting toxicity long before reaching an active concentration. In practice the observed profile is dominated by rash and stomatitis, with grade 3 or higher events in 43.6% of patients, lower than the 57.5% seen with chemotherapy in the same trial (O'Reilly et al., 2026; Wasko et al., 2024).

Why the window exists is not, in our view, adequately explained. The standard account invokes differential dependence, with RAS-addicted tumour cells more sensitive to a given degree of pathway suppression than normal tissue. That is consistent with the data but it is close to a restatement of the observation. Alternative contributions, from pharmacokinetic distribution to tumour-selective complex formation, have not been systematically dissected. The question is not academic: whether the window widens or narrows with more potent next-generation agents such as AN-9025 and GFH547 will determine how far this modality can be pushed, and a mechanistic answer would let that be predicted rather than discovered empirically.

5.3. Resistance is now informative rather than merely inconvenient

One under-appreciated consequence of having several mechanistically distinct modalities is that resistance patterns have become diagnostic. A Y96C substitution says something different from a Y64H, which says something different again from focal amplification or from a YAP/TAZ-driven transcriptional state (Awad et al., 2021; Sang et al., 2026; Wasko et al., 2024). Each points toward a different next move, as (Figure 5) and (Table 4) set out.

Two observations from the tri-complex resistance work seem particularly important. First, Y64 mutations disrupt the drug-chaperone interface rather than the nucleotide pocket, which means they can be engineered around: RMC-4791 preserves cyclophilin A recruitment through an altered binding geometry (Sang et al., 2026). Resistance to a molecular glue is, in that sense, a chemistry problem with a chemistry solution. Second, Y71H and class III BRAF alterations do not touch the drug at all; they raise the affinity of the native competitor (Sang et al., 2026). No amount of binder optimisation addresses that, and the implication is that effector-level combination will be necessary rather than optional for a subset of patients. The demonstration that GTP hydrolysis can be pharmacologically restored offers yet another axis, one that would sidestep the competition problem entirely (Cuevas-Navarro et al., 2025).

5.4. Where the pancreatic microenvironment complicates the picture

PDAC is where these agents matter most and where the biology is least forgiving. The desmoplastic stroma restricts drug delivery, the immune infiltrate is sparse and skewed toward suppression, and tumour cells sit in a metabolic environment that supports adaptation (Ahmed et

al., 2026; Alanazi et al., 2025). It is therefore notable that several RAS-directed agents appear to remodel this environment rather than merely surviving it, with MRTX1133 and ADT-1004 both shifting macrophage polarisation, depleting MDSCs, and increasing CD8+ infiltration (Bandi et al., 2025; Hallin et al., 2022).

We would flag an interpretive caution here. Whether these immune changes are a direct pharmacological effect of RAS pathway inhibition in tumour cells, or a downstream consequence of tumour regression producing antigen release and reduced immunosuppressive signalling, has not been cleanly resolved in most reports. The distinction determines whether checkpoint blockade should be given concurrently, to exploit a drug-induced window, or sequentially, after cytoreduction. The preclinical combination data are encouraging (Broderick et al., 2025; Orlen et al., 2025), but they do not settle the timing question, and the clinical trials now running should be designed to answer it rather than assuming it.

5.5. Limitations of this study and of the underlying evidence

Several constraints apply. Most clinical data cited here come from single-arm cohorts of twenty to sixty patients, with all the selection and regression-to-the-mean concerns that implies; only RASolute-302 and CodeBreaK 300 provide randomised comparison (Fakih et al., 2023; O'Reilly et al., 2026). Several datasets exist only as conference abstracts and have not been through full peer review (Arbour et al., 2023; Azad et al., 2026; Li et al., 2024; Spira et al., 2025). Follow-up across the active-state programmes is short, so durability and late toxicity remain unknown. Our own synthesis is narrative and therefore more vulnerable to interpretation bias than a quantitative one would be; we restricted to English-language records; and no protocol was registered. Publication bias almost certainly flatters the preclinical literature, since degrader and trapper programmes that failed are rarely reported. Finally, the pace of the field means that some conclusions drawn here will be superseded, quite possibly within the year.

5.6. Priorities that follow

Four seem clear to us. First, resistance-stratified trial design: with escape mechanisms now molecularly defined, allocating combination therapy by the alteration actually detected on serial ctDNA is achievable and would be more informative than empirical pairing (Chan et al., 2026; Sang et al., 2026). Second, mechanistic dissection of the pan-RAS therapeutic window, which currently rests on observation rather than understanding (Wasko et al., 2024). Third, systematic attention to non-genetic resistance, which is invisible to sequencing and may account for a substantial share of progressions attributed to unknown causes (Adachi et al., 2023; Singhal et al., 2024). Fourth, moving effective agents into earlier lines and into the adjuvant setting, where tumour burden is lower and clonal heterogeneity narrower, and where a drug that doubles survival in the metastatic setting might plausibly do considerably more (Wolpin et al., 2026).

6. Conclusion

RAS spent thirty years as the definitive undruggable target, and the judgement was reasonable on the evidence then available. What changed it was not better chemistry against the known structure but the recognition that druggability is a property of states rather than proteins. A cryptic pocket beneath Switch II opened the first route; abandoning the inactive state altogether opened the rest. Tri-complex molecular glues, targeted degraders, and nucleotide-free trappers now reach alleles and isoforms that covalent G12C chemistry never could, and randomised Phase III data support pan-RAS inhibition in pretreated metastatic pancreatic cancer with a tolerability profile better than chemotherapy. Resistance has followed, as it always does, but its architecture is now mapped well enough to be acted upon rather than merely observed. The remaining work is less about finding new binding modes than about deciding, for a given tumour, which escape route to close first.

References

Adachi, Y., Ito, K., Hayashi, Y., Kimura, R., Tan, T. Z., Yamaguchi, R., & Ebi, H. (2020). Epithelial-to-mesenchymal transition is a cause of both intrinsic and acquired resistance to KRAS G12C inhibitor in KRAS G12C-mutant non-small cell lung cancer. Clinical Cancer Research, 26(22), 5962–5973. https://doi.org/10.1158/1078-0432.CCR-20-2077

Adachi, Y., Kimura, R., Hirade, K., et al. (2023). Scribble mis-localization induces adaptive resistance to KRAS G12C inhibitors through feedback activation of MAPK signaling mediated by YAP-induced MRAS. Nature Cancer, 4(6), 829–843. https://doi.org/10.1038/s43018-023-00566-w

Ahmed, S., Ogilvie, T., Vizeacoumar, F. J., & Vizeacoumar, F. (2026). Precision oncology in pancreatic ductal adenocarcinoma: Targeted therapy advances. Current Oncology, 33(4), 452–480. https://doi.org/10.3390/curroncol33040452

Alanazi, F. E., Alatawi, Y., Alattar, A., Alshaman, R., Kotb, A. A., & Hetta, H. F. (2025). Broad-

spectrum RAS inhibition in pancreatic ductal adenocarcinoma: Mechanistic advances and therapeutic promise. Pharmaceuticals, 18(12), 1788. https://doi.org/10.3390/ph18121788

Arbour, K. C., Punekar, S. R., Garrido-Laguna, I., Hong, D. S., Wolpin, B., Pelster, M. S., ... & Chang, S. (2023). Preliminary clinical activity of RMC-6236, a first-in-class RAS(ON) multi-selective tri-complex inhibitor, in patients with RAS-mutant solid tumors. Annals of Oncology, 34, S458.

Aronchik, I., Kar, S., Zhuang, Y., et al. (2025). Resistance mechanisms to monotherapy RAS(ON) multi-selective inhibitor daraxonrasib (RMC-6236) in RAS mutant PDAC inform therapeutic combination strategies. Molecular Cancer Therapeutics, 24(10 Suppl), Abstract A081.

Awad, M. M., Liu, S., Rybkin, I. I., Arbour, K. C., Dilly, J., Zhu, V. W., Johnson, M. L., Heist, R. S., Patil, T., Riely, G. J., & Janne, P. A. (2021). Acquired resistance to KRAS(G12C) inhibition in cancer. New England Journal of Medicine, 384(25), 2382–2393. https://doi.org/10.1056/NEJMoa2105281

Azad, N. S., Kim, D., Oberstein, P., et al. (2026). Safety and efficacy of zoldonrasib (RMC-9805) plus daraxonrasib (RMC-6236) in patients with 2L+ KRAS G12D metastatic pancreatic adenocarcinoma (mPDAC). Annals of Oncology, 37(Suppl 2), S123–S124.

Bandi, D. S. R., Nagaraju, G. P., Sarvesh, S., Carstens, J. L., Foote, J. B., Graff, E. C., Fang, Y. D., Keeton, A. B., Chen, X., Valiyaveettil, J., & Piazza, G. A. (2025). ADT-1004: A first-in-class, oral pan-RAS inhibitor with robust antitumor activity in preclinical models of pancreatic ductal adenocarcinoma. Molecular Cancer, 24(1), Article 76. https://doi.org/10.1186/s12943-025-02276-8

Bekaii-Saab, T. S., Yaeger, R., Spira, A. I., Pelster, M., Sabari, J. K., Hafez, N., Barve, M., Velastegui, K., Yan, X., Shetty, A., & Janne, P. A. (2023). Adagrasib in advanced solid tumors harboring a KRAS G12C mutation. Journal of Clinical Oncology, 41(25), 4097–4106. https://doi.org/10.1200/JCO.23.00434

Bond, M. J., Chu, L., Nalawansha, D. A., Li, K., & Crews, C. M. (2020). Targeted degradation of oncogenic KRAS(G12C) by VHL-recruiting PROTACs. ACS Central Science, 6(8), 1367–1375.

Broderick, C., Mezzadra, R., Sisso, E. M., Mbuga, F., Raghulan, R., Chaves-Perez, A., Kulick, A., Jiang, L., Jiang, J., Ho, Y. J., & Lowe, S. W. (2025). A RAS(ON) multi-selective inhibitor combination therapy triggers long-term tumor control through senescence-associated tumor-immune equilibrium in pancreatic ductal adenocarcinoma. Cancer Discovery, 15(8), 1717–1739. https://doi.org/10.1158/2159-8290.CD-24-1185

Camps-Fajol, C., et al. (2025). Emerging concepts in targeting c-Myc and RAS/SOS1 interactions in human malignancies. Pharmacological Research, 211, Article 107544. https://doi.org/10.1016/j.phrs.2025.107544

Canon, J., Rex, K., Saiki, A. Y., Mohr, C., Cooke, K., Bagal, D., Gaida, K., Holt, T., Knutson, C. G., Koppada, N., & Lipford, J. R. (2019). The clinical KRAS(G12C) inhibitor AMG 510 drives anti-tumour immunity. Nature, 575(7781), 217–223. https://doi.org/10.1038/s41586-019-1694-1

Chan, L. L., Kwong, T. T., Yau, J. C. W., & Chan, S. L. (2026). RAS-targeted therapies for pancreatic cancer. ESMO Gastrointestinal Oncology, 8, Article 100096. https://doi.org/10.1016/j.esmogo.2026.100096

Choucair, K., Imtiaz, H., Uddin, M. H., Nagasaka, M., Al-Hallak, M. N., Philip, P. A., El-Rayes, B., Pasche, B. C., & Azmi, A. S. (2025). Targeting KRAS mutations: Orchestrating cancer evolution and therapeutic challenges. Signal Transduction and Targeted Therapy, 10, Article 385. https://doi.org/10.1038/s41392-025-02100-y

Cregg, J., Edwards, A. V., Chang, S., Lee, B. J., Knox, J. E., Tomlinson, A. C. A., Marquez, A., Liu, Y., Freilich, R., Aay, N., & Holderfield, M. (2025). Discovery of Daraxonrasib (RMC-6236), a potent and orally bioavailable RAS(ON) multi-selective, noncovalent tri-complex inhibitor for the treatment of patients with multiple RAS-addicted cancers. Journal of Medicinal Chemistry, 68(7), 6064–6083. https://doi.org/10.1021/acs.jmedchem.4c02314

Cuevas-Navarro, A., Pourfarjam, Y., Hu, F., Rodriguez, D. J., Vides, A., Sang, B., & Lito, P. (2025). Pharmacological restoration of GTP hydrolysis by mutant RAS. Nature, 637, 224–229. https://doi.org/10.1038/s41586-024-08200-1

Daley, B. R., Sealover, N. E., Finniff, B. A., et al. (2025). SOS1 inhibition enhances the efficacy of KRAS G12C inhibitors and delays resistance in lung adenocarcinoma. Cancer Research, 85(1), 118–133. https://doi.org/10.1158/0008-5472.CAN-24-1890

de Langen, A. J., Johnson, M. L., Mazieres, J., Dingemans, A. C., Mountzios, G., Pless, M., Wolf, J., Schuler, M., Lena, H., & Skoulidis, F. (2023). Sotorasib versus docetaxel for previously treated non-small-cell lung cancer with KRAS G12C mutation: A randomised, open-label, phase 3 trial. The Lancet, 401(10378), 733–746. https://doi.org/10.1016/S0140-6736(23)00078-4

Drizyte-Miller, K., Engstrom, L. D., Klomp, J. A., et al. (2025). Combination of the MTA-cooperative PRMT5 inhibitor BMS-986504 and KRAS inhibitors is an effective treatment strategy for MTAP-deleted KRAS-mutant pancreatic cancer. Cancer Research, 85(18), 3540–3557. https://doi.org/10.1158/0008-5472.CAN-25-0112

Edwards, A. C., Stalnecker, C. A., Jean Morales, A., et al. (2023). TEAD inhibition overcomes YAP1/TAZ-driven primary and acquired resistance to KRAS G12C inhibitors. Cancer Research, 83(24), 4112–4129. https://doi.org/10.1158/0008-5472.CAN-23-1180

Fakih, M. G., Salvatore, L., Esaki, T., Modest, D. P., Lopez-Bravo, D. P., Taieb, J., Karamouzis, M. V., Ruiz-Garcia, E., Kim, T. W., Kuboki, Y., & Kopetz, S. (2023). Sotorasib plus Panitumumab in refractory colorectal cancer with mutated KRAS G12C. New England Journal of Medicine, 389(23), 2125–2139. https://doi.org/10.1056/NEJMoa2308771

Habib, R., Arnold, E., Obi, T., Vizeacoumar, F. J., & Ahmed, S. (2026). Targeted therapy in pancreatic ductal adenocarcinoma: Current advances and challenges. Current Oncology, 33(4), Article 452. https://doi.org/10.3390/curroncol33040452

Hagenbeek, T. J., et al. (2023). Allosteric TEAD inhibitor GNE-7883 blocks oncogenic YAP/TAZ signaling and overcomes KRAS G12C inhibitor resistance. Nature Cancer, 4(6), 812–828. https://doi.org/10.1038/s43018-023-00565-x

Hallin, J., Bowcut, V., Calinisan, A., Briere, D. M., Hargis, L., Engstrom, L. D., Laguer, J., Medwid, J., Vanderpool, D., Lifset, E., & Christensen, J. G. (2022). Anti-tumor efficacy of a potent and selective non-covalent KRAS(G12D) inhibitor. Nature Medicine, 28(10), 2171–2182. https://doi.org/10.1038/s41591-022-02007-7

Holderfield, M., Lee, B. J., Jiang, J., Tomlinson, A., Seamon, K. J., Mira, A., Schulze, C. J., & Arbour, K. C. (2024). Concurrent inhibition of oncogenic and wild-type RAS-GTP for cancer therapy. Nature, 629(8013), 919–926. https://doi.org/10.1038/s41586-024-07388-6

Isermann, T., Sers, C., Der, C. J., & Papke, B. (2025). KRAS inhibitors: Resistance drivers and combinatorial strategies. Trends in Cancer, 11(2), 91–116. https://doi.org/10.1016/j.trecan.2024.11.004

Janes, M. R., Zhang, J., Li, L. S., Hansen, R., Peters, U., Guo, X., ... & Ren, P. (2018). Targeting KRAS mutant cancers with a covalent G12C-specific inhibitor. Cell, 172(3), 578–589.

Jiang, J., Jiang, L., Maldonato, B. J., Wang, Y., Holderfield, M., Aronchik, I., ... & Arbour, K. C. (2024). Translational and therapeutic evaluation of RAS-GTP inhibition by RMC-6236 in RAS-driven cancers. Cancer Discovery, 14(6), 994–1017.

Jiang, L., et al. (2025). Direct and indirect KRAS-targeting degraders in cancer therapy: Current progress and future perspectives. Bioorganic Chemistry, 166, 109161.

Jänne, P. A., Riely, G. J., Gadgeel, S. M., Heist, R. S., Ou, S. I., Pacheco, J. M., Johnson, M. L., Sabari, J. K., Leventakos, K., Yau, E., & Christensen, J. G. (2022). Adagrasib in non-small-cell lung cancer harboring a KRAS(G12C) mutation. New England Journal of Medicine, 387(2), 120–131. https://doi.org/10.1056/NEJMoa2204619

Kang, D., Wang, Y., Lin, Y., et al. (2025). JAB-3312, a potent allosteric SHP2 inhibitor that enhances the efficacy of RTK/RAS/MAPK and PD-1 blockade therapies. Clinical Cancer Research, 31(14), 3019–3032. https://doi.org/10.1158/1078-0432.CCR-24-2810

Li, J., Shen, L., Gu, Y., et al. (2024). Preliminary activity and safety results of KRAS G12C inhibitor glecirasib (JAB-21822) in patients with pancreatic cancer and other GI malignancies. Journal of Clinical Oncology, 42(16 Suppl), Abstract 4118.

O'Reilly, E. M., Wainberg, Z. A., Hendifar, A. E., Borad, M. J., Pietrantonio, F., Pant, S., Hammel, P., Cremolini, C., Manji, G. A., Oberstein, P. E., & Wolpin, B. M. (2026). Daraxonrasib or chemotherapy in previously treated metastatic pancreatic cancer. New England Journal of Medicine, 395(4), 325–337. https://doi.org/10.1056/NEJMoa2512398

Orlen, M., Vostrejs, W. P., Sor, R., et al. (2025). T-cell dependency of tumor regressions and complete responses with RAS(ON) multi-selective inhibition in preclinical models of pancreatic ductal adenocarcinoma. Cancer Discovery, 15(8), 1697–1716. https://doi.org/10.1158/2159-8290.CD-24-1050

Ostrem, J. M., Peters, U., Sos, M. L., Wells, J. A., & Shokat, K. M. (2013). K-Ras(G12C) inhibitors allosterically control GTP affinity and effector interactions. Nature, 503(7477), 548–551. https://doi.org/10.1038/nature12796

Pant, S., Ducreux, M. P., Ikeda, M., et al. (2026). A phase 2/3 randomized study of BMS-986504 with nab-paclitaxel and gemcitabine in first-line metastatic pancreatic ductal adenocarcinoma with homozygous MTAP deletion (MountainTAP-30). Journal of Clinical Oncology, 44(2 Suppl), TPS796.

Park, W., Kasi, A., Spira, A. I., et al. (2024). Preliminary safety and clinical activity of ASP3082, a first-in-class, KRAS G12D selective protein degrader in adults with advanced pancreatic, colorectal, and non-small cell lung cancer. Annals of Oncology, 35, S486–S487.

Park, W., Kasi, A., Spira, A. I., et al. (2026). Setidegrasib in advanced non-small-cell lung cancer and pancreatic cancer. New England Journal of Medicine, 394(14), 1409-1420.

Patel, R. P., et al. (2025). Sensitivity to immune checkpoint inhibitors in BRAF/MEK inhibitor refractory melanoma. Journal for ImmunoTherapy of Cancer, 13(2), e011551. https://doi.org/10.1136/jitc-2024-011551

Popow, J., Farnaby, W., Gollner, A., Kofink, C., Fischer, G., Wurm, M., ... & Kraut, N. (2024). Targeting cancer with small-molecule pan-KRAS degraders. Science, 385(6715), 1338–1347.

Prior, I. A., Hood, F. E., & Hartley, J. L. (2020). The frequency of Ras mutations in cancer. Cancer Research, 80(14), 2969–2974.

Sacher, A., LoRusso, P., Patel, M. R., Miller, W. H., Garralda, E., Forster, M. D., Santoro, A., Falcon, A., Kim, T. W., Paz-Ares, L., & Garon, E. B. (2023). Single-agent divarasib (GDC-6036) in solid tumors with a KRAS G12C mutation. New England Journal of Medicine, 389(8), 710–721. https://doi.org/10.1056/NEJMoa2308000

Sang, B., Ye, L. F., Fu, Z., et al. (2026). Disrupted molecular glue complex drives RAS inhibitor resistance. Cell, 189(10), 2918–2933. https://doi.org/10.1016/j.cell.2026.04.015

Schulze, C. J., Seamon, K. J., Zhao, Y., Yang, Y. C., Cregg, J., Kim, D., Tomlinson, A., Choy, T. J., Wang, Z., Sang, B., & Holderfield, M. (2023). Chemical remodeling of a cellular chaperone to target the active state of mutant KRAS. Science, 381(6659), 794–799. https://doi.org/10.1126/science.add8687

Singhal, A., Styers, H. C., Rub, J., et al. (2024). A classical epithelial state drives acute resistance to KRAS inhibition in pancreatic cancer. Cancer Discovery, 14(11), 2122–2134. https://doi.org/10.1158/2159-8290.CD-24-0158

Skoulidis, F., Li, B. T., Dy, G. K., Price, T. J., Falchook, G. S., Wolf, J., Italiano, A., Schuler, M., Borghaei, H., Barlesi, F., & Ramalingam, S. S. (2021). Sotorasib for lung cancers with KRAS p.G12C mutation. New England Journal of Medicine, 384(25), 2371–2381. https://doi.org/10.1056/NEJMoa2103695

Spira, A. I., Papadopoulos, K. P., Kim, D. W., et al. (2025). Preliminary safety, antitumor activity, and circulating tumor DNA (ctDNA) changes with RMC-9805, an oral, RAS(ON) G12D-selective tri-complex inhibitor in patients with KRAS G12D pancreatic ductal adenocarcinoma (PDAC) from a phase 1 study in advanced solid tumors. Journal of Clinical Oncology, 43(4 Suppl), Abstract 724. https://doi.org/10.1200/JCO.2025.43.4_suppl.724

Strickler, J. H., Satake, H., George, T. J., Yaeger, R., Hollebecque, A., Garrido-Laguna, I., Schuler, M., Burns, T. F., Coveler, A. L., Falchook, G. S., & Fakih, M. G. (2023). Sotorasib in KRAS p.G12C-mutated advanced pancreatic cancer. New England Journal of Medicine, 388(1), 33–43. https://doi.org/10.1056/NEJMoa2208470

Tanaka, N., Lin, J. J., Li, C., et al. (2021). Clinical acquired resistance to KRAS G12C inhibition through a novel KRAS switch-II pocket mutation and polyclonal alterations converging on RAS–MAPK reactivation. Cancer Discovery, 11(8), 1913–1922. https://doi.org/10.1158/2159-8290.CD-21-0365

Wang, L., Jiang, K., Li, W., et al. (2025). HRS-4642 combined with gemcitabine and nab-

paclitaxel in KRAS-G12D mutant advanced pancreatic cancer: A phase Ib/II study. Annals of Oncology, 36(Suppl 8), S1146.

Wang, X., Allen, S., Blake, J. F., Bowcut, V., Briere, D. M., Calinisan, A., Dahlke, J. R., Fell, J. B., Fischer, J. P., Gunn, R. J., & Christensen, J. G. (2022). Identification of MRTX1133, a noncovalent, potent, and selective KRAS(G12D) inhibitor. Journal of Medicinal Chemistry, 65(4), 3123–3133. https://doi.org/10.1021/acs.jmedchem.1c01688

Wasko, U. N., Jiang, J., Dalton, T. C., et al. (2024). Tumour-selective activity of RAS-GTP inhibition in pancreatic cancer. Nature, 629(8013), 927–936. https://doi.org/10.1038/s41586-024-07379-7

Wolpin, B. M., Musher, B. L., Manji, G. A., Park, W., Spira, A., Azad, N., Florou, V., De Castria, T. B., O'Hara, M. H., Borazanci, E., & O'Reilly, E. M. (2026). Daraxonrasib plus chemotherapy as first-line treatment for patients with metastatic pancreatic adenocarcinoma. In Proceedings of the 2026 AACR Annual Meeting, Abstract LB407/7.

Yaeger, R., Weiss, J., Pelster, M. S., Spira, A. I., Barve, M., Ou, S. I., Leal, T. A., Bekaii-Saab, T. S., Paweletz, C. P., Heavey, G. A., & Kopetz, S. (2023). Adagrasib with or without Cetuximab in colorectal cancer with mutated KRAS G12C. New England Journal of Medicine, 388(1), 44–54. https://doi.org/10.1056/NEJMoa2212419

Yoshinari, T., Nagashima, T., Ishioka, H., Inamura, K., Nishizono, Y., Tasaki, M., Iguchi, K., Suzuki, A., Sato, C., Nakayama, A., & Yamanaka, Y. (2025). Discovery of KRAS(G12D) selective degrader ASP3082. Communications Chemistry, 8(1), Article 254. https://doi.org/10.1038/s42004-025-01654-2

Zhao, Y., Murciano-Goroff, Y. R., Xue, J. Y., Ang, A., Lucas, J., Mai, T. T., Da Cruz Paula, A. F., Saiki, A. Y., Mohn, D., Achanta, P., & Lito, P. (2021). Diverse alterations associated with resistance to KRAS(G12C) inhibition. Nature, 599(7886), 679–683. https://doi.org/10.1038/s41586-021-04065-2

Zhong, Q., Zhou, X., Meng, X., Sun, L., et al. (2025). Efficacy and safety of KRAS G12C inhibitor glecirasib combined with sitneprotafib in patients with advanced solid tumors. Journal of Thoracic Oncology, 20(3), 1630–1639.

Zhou, C., Fan, Z., Gu, Y., Ge, Z., Tao, Z., Cui, R., & Huo, R. (2024). Design, synthesis, and biological evaluation of potent and selective PROTAC degraders of oncogenic KRAS(G12D). Journal of Medicinal Chemistry, 67(2), 1147–1167. https://doi.org/10.1021/acs.jmedchem.3c01824